UNIVERSITE KASDI MERBAH OUARGLA

FACULTE DES SCIENCES APPLIQUEES

DEPARTEMENT DE GENIE MECANIQUE

N°d'ordre :
N° de série :

Mémoire

présenté pour l'obtention du diplôme de

Spécialité : Génie mécanique
Option : énergétique

Présenté par :

AFFANE Boudkhil

Thème

Développement d'un outil d'optimisation multicritère des systèmes solaires thermiques pour des besoins d'une habitation

Soutenu publiquement le : 09/06/2014

Devant le jury composé de :

Mme.	N.Saifi	MAA	Président	Université Kasdi Merbah Ouargla
Mr.	H.Belahia	MAA	Examinateur	Université Kasdi Merbah Ouargla
Mr.	B.Negrou	MAA	Encadreur	Université Kasdi Merbah Ouargla

Année universitaire: 2013/2014

KASDI MERBAH UNIVERSITY OUARGLA

FACULTY OF APPLIED SCIENCES

MECHANICAL ENGINEERING DEPARTMENT

N ° :
Serial No. :

Thesis

presented for Master graduation

Branch: mechanical Engineering
Option: energetic

Approved by:

Boudkhil AFFANE

Thesis

Development of an optimization code of solar thermal systems for residential requirements

Publicly supported on: 9/6/2014

Front of the committee members:

Mrs.	N.Saifi	AAP	President	Kasdi Merbah University Ouargla
Mr.	H.Belahia	AAP	Examiner	Kasdi Merbah University Ouargla
Mr.	B.Negrou	AAP	Advisor	Kasdi Merbah University Ouargla

ACADEMIC YEAR : 2013/2014

Acknowledgments

Thank Allah first place, the Almighty.

Foremost, I would like to express my sincere gratitude to my advisor Mr. B. Negrou for the continuous support of my Master study and research, for his patience, motivation, enthusiasm, and immense knowledge.

I would like to thank my kind family members, my father, my mother for their unstinting loyalty and support. I also extend a note of appreciation to Professor N.Settou for his support and encouragement and all the members of the thesis committee Mrs N.Saifi and Mr H.Belahia.

I would like to thank B.Rsioui, S.Rahmouni and all VPRS's laboratory members for their help and encouragement.

Last but not the least, I would like to thank all friends and people who helped and supported me spiritually throughout my life.

Summary

Nomenclature

Symbol	*Description*	*Unit*
f	*Solar fraction*	*[-]*
f_{tl}	*Total fraction of the monthly load supply by solar energy*	*[-]*
L_{tot}	*Total monthly heat demand*	*[J]*
Q_s	*Storage tank losses for month*	
X	*Modified sensibility factor of the thermal losses*	*[-]*
$\bar{X}_c$	*Dimensionless average daily critical level of the solar collector*	*[-]*
$\bar{X}_{c,min}$	*Minimum of the dimensionless average daily critical level of the solarcollector*	*[-]*
Y	*Ratio of the absorbed solar energy to the cooling load*	*[-]*
$\bar{\Phi}_{max}$	*Maximum monthly average daily utilizability*	*[-]*
$\bar{\Phi}$	*Monthly average daily collector utilizability*	*[-]*
A_C	*Collector area*	*[M²]*
C_P	*Specific heat capacity*	
C_{min}	*Minimum capacitance of the two fluid stream in the heat exchanger*	
(U_S)	*Overall loss coefficient-area product of the storage tank*	*[W/K]*
U_L	*Collector overall energy loss coefficient*	*[W/m²K]*
ε_L	*Effectiveness of the load heat exchanger*	*[-]*
Δt	*Total number of seconds in a month*	*[S]*
Δt_h	*Number of seconds during a month the load is required*	*[S]*
$\overline{(\tau\alpha)}$	*Monthly average energy transmittance–absorptance product*	*[-]*
$(\tau\alpha)_n$	*Transmittance–absorptance product for radiation at normal incidence*	*[-]*
F_R	*Collector overall heat removal efficiency factor*	*[-]*
F'_R	*Corrected F_R factor*	*[-]*
$\bar{H}$	*Monthly average daily total solar radiation on a horizontal surface*	*[Jm^{-2}]*
$\bar{H}_0$	*Monthly average daily extraterrestrial solar radiation*	*[Jm^{-2}]*
$\bar{H}_t$	*Monthly average daily total solar radiation on the collector surface*	*[Jm^{-2}]*
$\bar{K}_T$	*Clearness index*	*[-]*
L	*Heat required*	*[J]*
L_{req}	*Process required heat rate*	*[J]*
L_{tot}	*Total monthly heat demand*	*[J]*
M	*Actual mass of storage capacity*	*[kg]*
N	*Numbers of days in a month*	
Q_s	*Storage tank losses for month*	*[J]*
r_n	*Ratio of the diffuse solar radiation at solar noon to the*	*[-]*

	daily total radiation on a horizontal surface	
$\overline{R}$	*Ratio of the monthly average daily total radiation on a tilted surface to that on a horizontal surface*	***[-]***
R_n	*Ratio of radiation on a tilted surface to that on a horizontal surface at noon*	***[-]***
R_S	*Ratio of standard storage heat capacity per unit of collector area of 350 kJ/m²-°C to actual storage capacity*	***[-]***
$\overline{T}_a$	*Ambient temperature*	***[°C]***
T_i	*Inlet collector fluid temperature*	***[°C]***
T_{min}	*Minimum required temperature*	***[°C]***
$T_{p,min}$	*Useful energy temperature*	***[°C]***
$\overline{T}_S$	*Monthly average storage tank temperature*	***[°C]***
$T_{s,env}$	*Environment storage temperature*	***[°C]***

Figures List

Tables list

General Introduction

The use of renewable energy creates more of interest in the world. Decreasing global reserves of oil and gas, environmental problems have led many countries to focus on renewable and clean energy, such as solar thermal, which is one of the most easily exploitable. It is also inexhaustible. Its applications are numerous and varied, space heating and cooling, water heating, crop drying and solar cooking. It is a technology which is well understood and widely used in many countries throughout the world. Most solar thermal technologies have been in existence in one form or another for centuries and have a well-established manufacturing base in most sun-rich developed countries.

The most common use for solar thermal technology is for domestic water heating. Hundreds of thousands of domestic hot water systems are in use throughout the world, especially in areas such as the Mediterranean, as well as Algeria, where there is high solar insolation (the total energy per unit area received from the sun). As world oil prices vary, it is a technology which is rapidly gaining acceptance as an energy saving measure in both domestic and commercial water heating applications. Presently, domestic water heaters are usually only found amongst wealthier sections of the community in developing countries. The thermal solar system is a process made up of a solar collector, an actuator allowing the circulation of the coolant, and of a storage tank. Solar energy is collected by the absorbing surface of the solar collector.

The performance of all solar energy systems depends on the weather factors (level and distribution of isolation, ambient temperature), solar system parameters (collector type, storage capacity) and load characteristics (space heating, water heating, temperature level).

Among the most usual methods for designing and estimating the performances of the solar thermal systems are the methods known as the utilizability and f-Chart. The design method used in this master thesis's the $\overline{\Phi}, f$-chart method which is a combination of the utilizability and f-chart methods. The f-chart method is based on the correlation of the results of a large number of simulations in terms of easily calculated dimensionless variables [1]. The utilizability method is used in cases where the collector operating temperature is known or can be estimated and for which critical radiation levels can be established [2]. The utilizability method is based on the analysis of hourly weather data to obtain the fraction of the total month's radiation that is above a critical level. The $\overline{\Phi}, f$-chart method is a combination of the utilizability method and f-chart methods, applied in systems where the energy supplied to load is above a minimum useful temperature and the temperature of this energy supply has no effect on the performance of the load system as long as it is greater than the minimum temperature.

The most important concern in the design of solar heating systems is the optimal solar collector area which is defined as the area that optimizes the system from both economic and parametric viewpoints. This area is the result of a cost- benefit approach. The cost of the solar system and benefits of saving of the cost of auxiliary fuel accruing from the installation of the system.

The most important concern in the design of active solar/auxiliary heating systems is the optimal solar collector area which is defined as the area that optimizes the system from both economic. This area is the result of a cost- benefit approach. The cost of the solar system and benefits of saving of the cost of auxiliary fuel accruing from the installation of the system. In this work we introduced a mathematical model for the determination of optimal collector area of the solar installations of collective water heating. This method is based on a minimization of the total cost of the installation. This by holding account, not only costs of the various components and price of the conventional energy consumed by the auxiliary system, but also of the thermal performances of the installation starting from the F-Chart method.

This master thesis is divided into two complementary chapters:

In the first chapter we take an overview of solar thermal energy, and its various applications, a short description of solar water heating systems, we outline the f-chart method for estimating the annual thermal performance of active heating systems for buildings, the monthly average hourly utilizability (the φ method)for flat-plate collectors, then we show briefly how combined daily utilizability with the f-chart concept to account for finite storage capacity (the $\bar{\Phi}, f$-chart method).

In the second chapter we show how to implement the φ-f chart method for optimize the design of active solar heating systems using Scilab to develop a calculate module. The physical model used to calculate the solar fraction for hot water production with respect to the global request. This Scilab code can be used to estimate the thermal performance of solar energy systems for domestic water, industrial process heating, and space heating systems where the thermodynamics cycle efficiency is independent of the heat supply temperature. We also integrated a mathematical model for the determination of optimal collector area of the solar installations of collective water heating. This method is based on a minimization of the total cost of the installation. This by holding account, not only costs of the various components and price of the conventional energy consumed by the auxiliary system, but also of the thermal performances of the installation starting from the-f chart method.

Finally, a general conclusion which we suggest some recommendations.

Chapter I: Bibliographic Review

1. Introduction

The use of renewable energy creates more of interest in the world. Decreasing global reserves of oil and gas, environmental problems have led many countries to focus on renewable and clean energy, such as solar energy. This energy is one of the most easily exploitable. In this chapter we introduce the thermal solar energy, in particular the production of hot water, and a various design methods of the thermal solar systems. We also describe and model the φ-f chart method with Scilab. The φ-f chart method is a simulation technique used in solar energy systems for heating and cooling. This method is particularly useful for sizing system components. The difficulty of sizing system's components lies in the fact that these systems are influenced both by predictable data (e.g. collectors, storage tanks, …) and unpredictable data such as weather data. The method is applied to the closed loop solar energy system which is particularly useful in the simulation of absorption refrigerators, industrial process heating, and space heating systems where the thermodynamics cycle efficiency is independent of the heat supply temperature.

2. Solar thermal systems

2.1 The sun

The sun is a sphere of intensely hot gaseous matter with a diameter of 1.39×10^9m. The solar energy strikes our planet a mere 8 min and 20 s after leaving the giant furnace, the sun which is $\times 1.5 \times 10^9 m$ away. The sun has an effective blackbody temperature of 5762K. The temperature in the central region is much higher and it is estimated at 8×10^6K to40×10^6K. In effect the sun is a continuous fusion reactor in which hydrogen is turned into helium. The sun's total energy output is 3.8×10^{20}MW which is equal to 63 MW/m² of the sun's surface. This energy radiates outwards in all directions. Only a tiny fraction,$1.7 \times 10^{14} kW$, of the total radiation emitted is intercepted by the earth . However, even with this small fraction it is estimated that 30 min of solar radiation falling on earth is equal to the world energy demand for one year. [3]

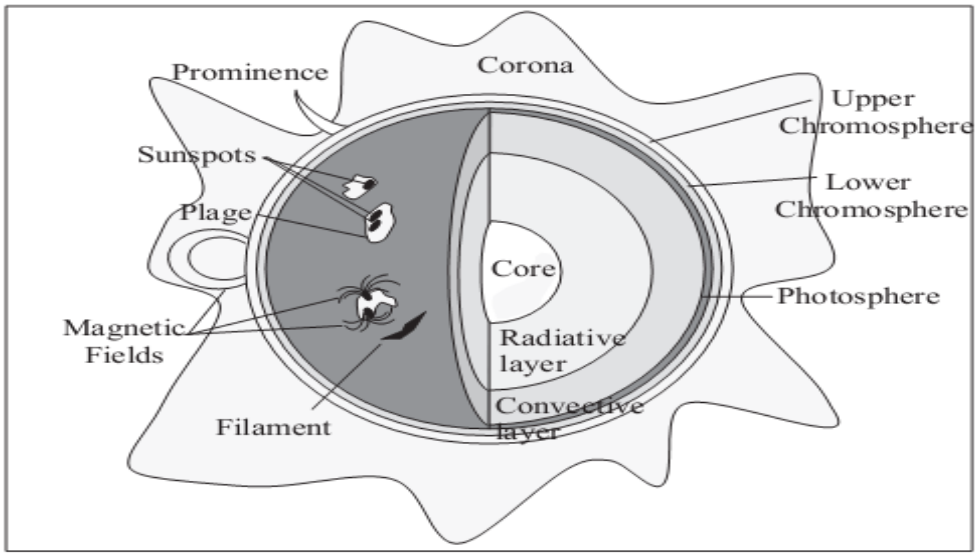

Figure I.1: The structure of the Sun [4].

2.2 Solar thermal energy

Solar thermal energy is the direct use of solar energy. It is the instantaneous conversion of sunlight energy into thermal energy. This transformation can be used directly as domestic hot water using solar collectors, or indirectly in the case of producing electricity in a solar thermodynamic plant.

Solar thermal energy has many applications:

- domestic hot water;
- home heating;
- heating swimming pool water;
- crop drying;
- absorption refrigeration for buildings;
- producing high temperature.

2.3 Solar thermal system

Solar thermal systems are a clean technology. They are silent, and can easily be integrated and are not pollutants. They have few moving parts and work relative to other technologies, at low temperature, which has the effect of lengthening their life, most of them can be renewed or recycled after 20-30 years of operation.

Solar Thermal Energy does not cause pollution which is one of the biggest advantages. Note there are costs associated with the equipment used to build and transport Solar Thermal Energy Equipment [5].

Solar Thermal System is one of most cost-effective renewable energy systems. Solar thermal systems are designed to collect or absorb solar energy for heating water used in residential, commercial and industrial applications. Solar thermal systems use different type

of collector to gather and store the solar energy. The system reduces the amount of electricity, gas or fuel required to heat water.

The thermal solar system is a process made up of a solar collector, an actuator allowing the circulation of the coolant, and of a storage tank. Solar energy is collected by the absorbing surface of the solar collector.

In what follows we will talk about one of the use of these systems is the production of hot water.

3. Solar Water Heating Background

3.1 Service hot water

For hot water production there are a number of service hot water applications. The most common application is the use of domestic hot water systems (DHWS), generally sold as “off-the-shelf” or standard kits

Figure I.2: Solar water heaters now mandatory in Hawaii, by JUSTIN THOMAS.

Other common uses include providing process hot water for commercial and institutional applications, including multi-unit houses and apartment buildings, as depicted in Figure I.2, housing developments, and in schools, health centers, hospitals, office buildings, restaurants and hotels.

3.2 Description of Solar Water Heating Systems

Solar water heating systems use solar collectors and a liquid handling unit to transfer heat to the load, generally via a storage tank. The liquid handling unit includes the pump(s) (used to circulate the working fluid from the collectors to the storage tank) and control and

safety equipment. When properly designed, solar water heaters can work when the outside temperature is well below freezing and they are also protected from overheating on hot, sunny days. Many systems also have a back-up heater to ensure that all of a consumer's hot water needs are met even when there is insufficient sunshine. Solar water heaters perform three basic operations as shown in Figure I.4:

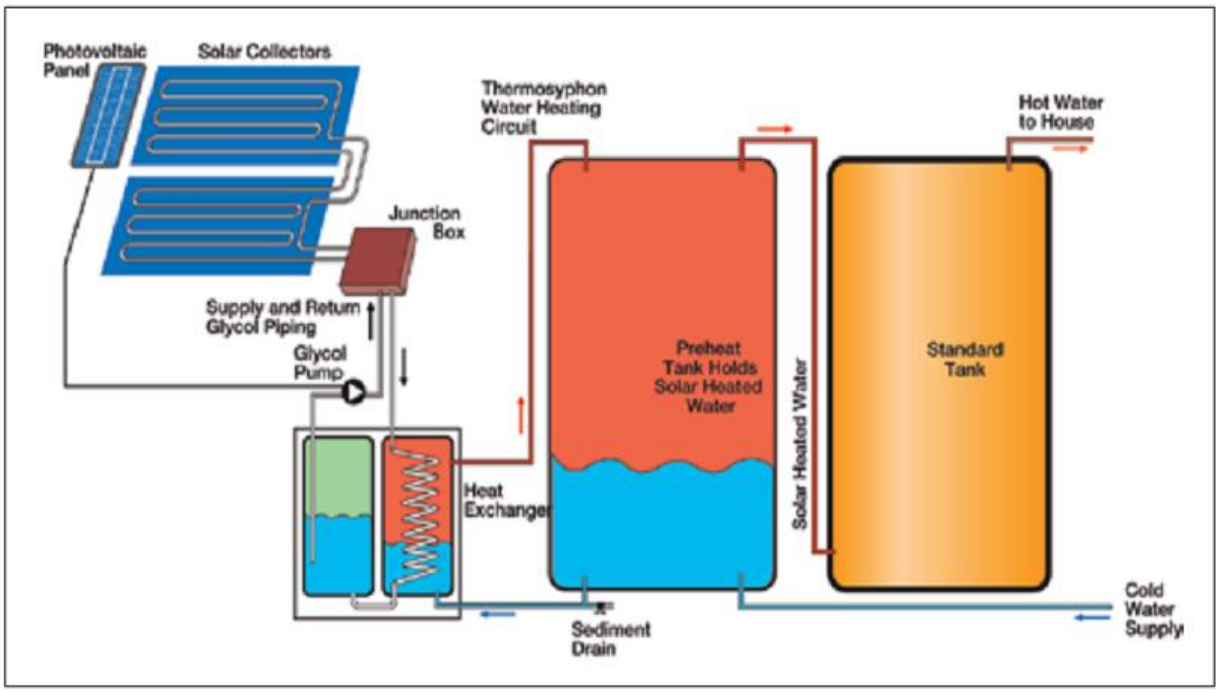

Figure I.4: System Schematic for Typical Solar Domestic Water Heater [10].

- **Collection:** Solar radiation is "captured" by a solar collector;
- **Transfer:** Circulating fluids transfer this energy to a storage tank; circulation can be natural (thermosiphon systems) or forced, using a circulator (low-head pump);
- **Storage:** Hot water is stored until it is needed at a later time in a mechanical room, or on the roof in the case of a thermosiphon system.

3.3 Solar collectors

The major component of any solar system is the solar collector. This device that absorbs the incoming solar radiation, converts it into heat, and transfers the heat to a fluid (usually air, water, or oil) flowing through the collector. The solar energy collected is carried from the circulating fluid either directly to the hot water or space conditioning equipment or to a thermal energy storage tank.

3.4 Different types of thermal solar collectors

There are several types of solar collectors to heat liquids. Selection of a solar collector type will depend on the temperature of the application being considered and the intended season of use (or climate). The most common solar collector types are: unglazed liquid flat-plate collectors; glazed liquid flat-plate collectors; and evacuated tube solar collectors.

3.4.1 Glazed liquid flat-plate collector

The most common collector used for hot water preparation and for space heating in world is the flat-plate collector. The flat-plate collector consists essentially of the collector box, the absorber, heat insulation and transparent cover.

Figure I.5: Glazed liquid flat-plate collector [13].

Flat-plate collectors use both beam and diffuse sola r radiation, do not require tracking of the sun, are low-maintenance, inexpensive and mechanically simple. Solar radiation enters the collector through the transparent cover and reaches the absorber. Here the absorbed radiation is converted to thermal energy. A good thermal conductivity is needed to transfer the collected heat from the absorber sheet to the absorber pipes where the heat is finally transferred to the fluid. Usually a water/glycol mixture with anticorrosion additives is used as the heat carrying fluid. The fluid also protects the collector from frost damage.

3.4.2 Unglazed liquid flat-plate collectors

Unglazed liquid flat-plate collectors, as depicted in Figure I-6, are usually made of a black polymer. They do not normally have a selective coating and do not include a frame and insulation at the back; they are usually simply laid on a roof or on a wooden support. These low-cost collectors are good at capturing the energy from the sun, but thermal losses to the environment increase rapidly with water temperature particularly in windy locations.

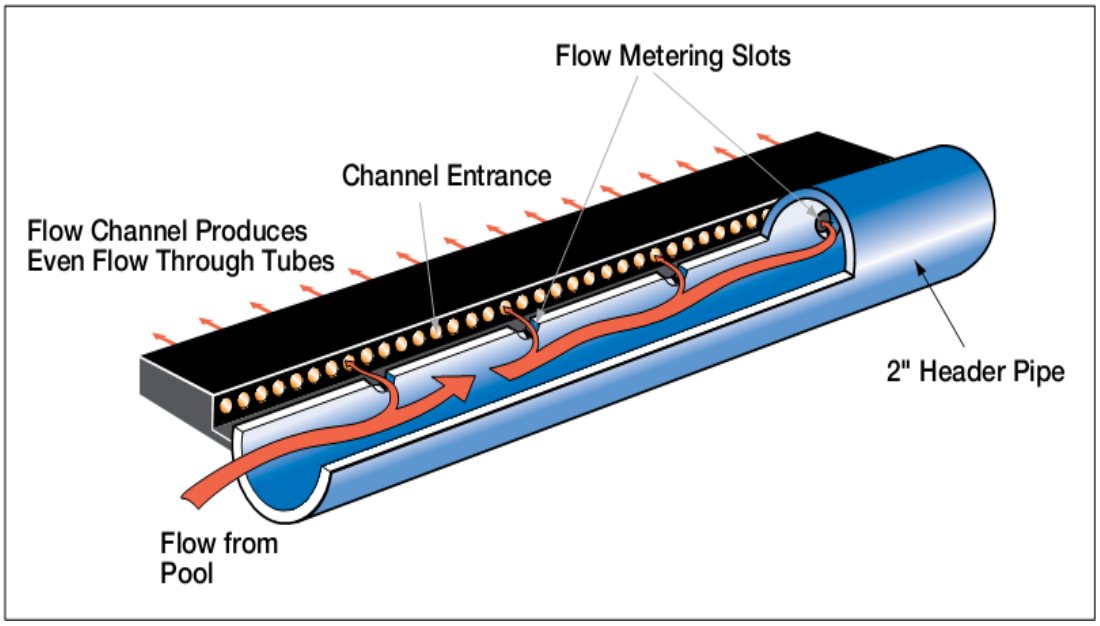

Figure I.6: system schematic for unglazed flat-plate solar collector [10].

As a result, unglazed collectors are commonly used for applications requiring energy delivery at low temperatures (pool heating, make-up water in fish farms, process heating applications, and etc. figure I-7); in colder climates they are typically only operated in the summer season due to the high thermal losses of the collector.

Figure I.7: Unglazed liquid flat-plate collector [14]

3.4.3 Evacuated tube solar collectors

Evacuated tube solar collectors, as depicted in Figure I-8, have an absorber with a selective coating enclosed in a sealed glass vacuum tube. They are good at capturing the energy from the sun; their thermal losses to the environment are extremely low. Systems presently on the market use a sealed heat-pipe on each tube to extract heat from the absorber (a liquid is vaporized while in contact with the heated absorber, heat is recovered at the top of the tube while the vapor condenses, and condensate returns by gravity to the absorber).

Evacuated collectors are good for applications requiring energy delivery at moderate to high temperatures (domestic hot water, space heating and process heating applications typically at 60°C to 80°C depending on outside temperature), particularly in cold climates.

Figure I.8: Evacuated tube solar collectors [7].

4. Solar energy calculation

For evaluating solar energy, it is necessary to know the distribution of solar radiation on the location planned for the installation under different inclinations. However, solar radiation is one of the most difficult meteorological parameters to estimate, because it depends on many geographical and astronomical parameters.

Since the solar water heating model deals with solar energy, some basic concepts of solar energy engineering first needs to be explained.

4.1 Declination

The declination is the angular position of the sun at solar noon, with respect to the plane of the equator. Its value in degrees is given by Cooper's equation [6]:

$$\delta = 23.45° \, sin\left[2\pi \frac{284+n}{365}\right] \quad \text{(I-1)}$$

Where:

δ The declination (°)
n Day number of the year from January 1

Declination varies between -23.45 ° (21 December) and +23.45 ° (June 21).

4.2 True solar time

True solar time is defined from the rotation of the earth on itself. It is therefore directly related to the hour angle. The earth makes a complete rotation in 24 hours. It is noon (12h) when the sun is at its zenith, it's given by [18]:

$$TSV = 12 - \frac{\omega}{15} \quad \text{(I-2)}$$

ω Hour angle (°)

4.3 The hour angle

The hour angle, ω, is the angular distance between the meridian of the observer and the meridian whose plane contains the sun. Thus, the hour angle is zero at local noon (when the sun reaches its highest point in the sky). At this time the sun is said to be 'due south' (or 'due north', in the Southern Hemisphere) since the meridian plane of the observer contains the sun. The hour angle increases by 15 degrees every hour [8].

4.4 Sun position

4.4.a Angle of solar elevation (h) : it can be shown that the angle of solar elevation ,h , may be expressed in terms of the Sun's declination angle, δ, on a given date, the current hour angle(i.e the time of day) ω , and observer's latitude , ψ , via equation:

$$sin(h) = sin(\psi)sin(\delta) + cos(\psi)cos(\delta)cos(\omega) \quad \text{(I-3)}$$

Sunrise hour angle (ω_s) is obtained by writing $sin(h) = 0$ [8]:

$$cos\,\omega_s = -tan(\psi)tan(\delta) \quad \text{(I-4)}$$

ω Hour angle (°)
ψ The latitude of a specified location on Earth (°)

4.4.b Solar azimuth (a) : The azimuth angle is the compass direction from which the sunlight is coming. At solar noon, the sun is always directly south in the northern hemisphere and directly north in the southern hemisphere, it's given by:

$$\sin(a) = \cos(\delta)\sin(\omega)/\cos(h) \quad \text{(I-5)}$$

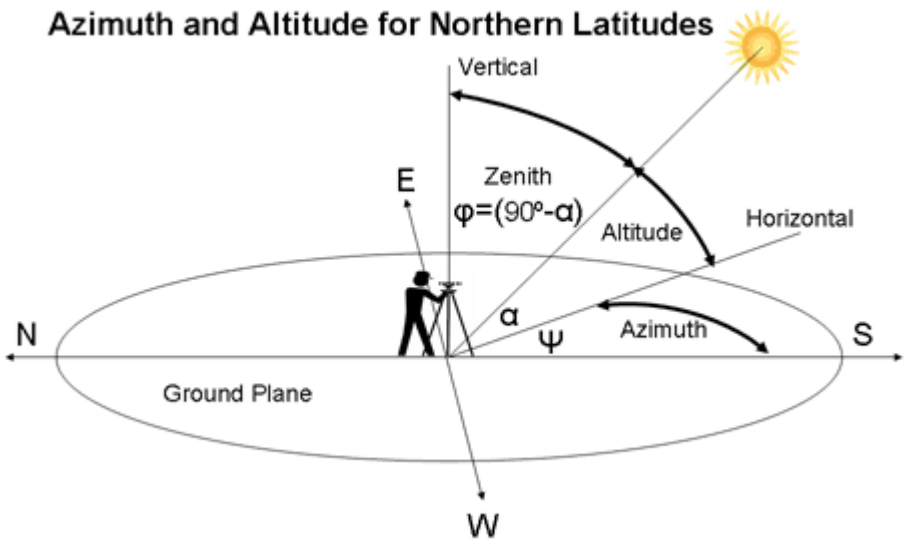

Figure I.10: Sun position [12].

4.5 Extraterrestrial radiation and clearness index

The extraterrestrial solar radiation is a function of the solar constant G_{sc} and correction of the distance between the earth and the sun. The solar constant is the energy flux received by a unit area. The value was chosen in 1980: G_{sc} = 1367 (W/m²).

For n given day, the extraterrestrial radiation on a horizontal surface can be calculated by:

$$H_0 = \frac{24\times3600}{\pi} G_{sc}\left(1 + 0.0033\cos 2\pi\frac{n}{365}\right)(\cos\psi\cos\delta\cos\omega_s + \sin\psi\sin\delta) \qquad \text{(I-6)}$$

Before reaching the surface of the earth, radiation from the sun is attenuated by the atmosphere and the clouds. The ratio of solar radiation at the surface of the earth to extraterrestrial radiation is called the clearness index. Thus the monthly average clearness index, $\overline{K}_T$ is defined as:

$$\overline{K}_T = \frac{\overline{H}}{\overline{H}_0} \qquad \text{(I-7)}$$

Where $\overline{H}$ is the monthly average daily solar radiation on a horizontal surface and $\overline{H}_0$ is the monthly average extraterrestrial daily solar radiation on a horizontal surface. $\overline{K}_T$ values depend on the location and the time of year considered; they are usually between 0.3 (for very overcast climates) and 0.8 (for very sunny locations)[10].

4.6 Tilted irradiance

Solar radiation in the plane of the solar collector is required to estimate the efficiency of the collector and the actual amount of solar energy collected.

$$\overline{H}_T = \overline{H}_b.\overline{R}_b + \overline{H}_d\left(\frac{1+\cos\beta}{2}\right) + \overline{H}.\rho.\left(\frac{1-\cos\beta}{2}\right) \qquad \text{(I-8)}$$

The first term on the right-hand side of this equation represents solar radiation coming directly from the sun. It is the product of monthly average beam radiation $\overline{H}_b$ times a purely geometrical factor, $\overline{R}_b$, which depends only on collector orientation, site latitude, and time of year. The second term represents the contribution of monthly average diffuse radiation, $\overline{H}_d$, which depends on the slope of the collector,β . The last term represents reflection of radiation on the ground in front of the collector, and depends on the slope of the collector and on ground reflectivity, ρ_g . This latter value is assumed to be equal to 0.2 when the monthly average temperature is above 0°C and 0.7 when it is below -5°C; and to vary linearly with temperature between these two thresholds.

Geometrical factor given by the following equation:

$$\overline{R}_b = \frac{cos(\psi-\beta).cos\,\delta.sin\,\omega_s{}'+\omega_s{}'.sin(\psi-\beta)\,sin\,\delta}{cos\psi\,.cos\,\delta.sin\,\omega_s+\omega_s.sin\,\psi\,sin\,\delta} \quad \text{(I-9)}$$

ω_s sunset hour angle on the horizontal level (°)
$\omega_s{}'$ sunset hour angle on the tilted level (°),

$$\omega_s{}' = Min[\omega_s\, cos^{-1}(-\,tan(\psi-\beta)\,tan\,\delta)]$$

5. Hot water system designing

5.1The f-chart method

5.1.1 Method description:

The f-chart method for estimating the annual thermal performance of active heating systems for buildings (using either liquid or air as the working fluid) where the minimum temperature of energy delivery is near 20°C. The system configurations that can be evaluated by the f-chart methods are expected to be common in residential applications.

Two dimensionless parameters X and Y are defined:

$$X = F_R U_L \times \frac{F'_R}{F_R} \times \left(T_{ref} - \bar{T}_a\right) \times \Delta t \times \frac{A_c}{L_{tot}} \quad \text{(I-10)}$$

$$Y = F_R(\overline{\tau\alpha}\,) \times \frac{F'_R}{F_R} \times \frac{(\overline{\tau\alpha}\,)}{(\tau\alpha\,)_n} \times \bar{H}_T N \times \frac{A_c}{L_{tot}} \quad \text{(I-11)}$$

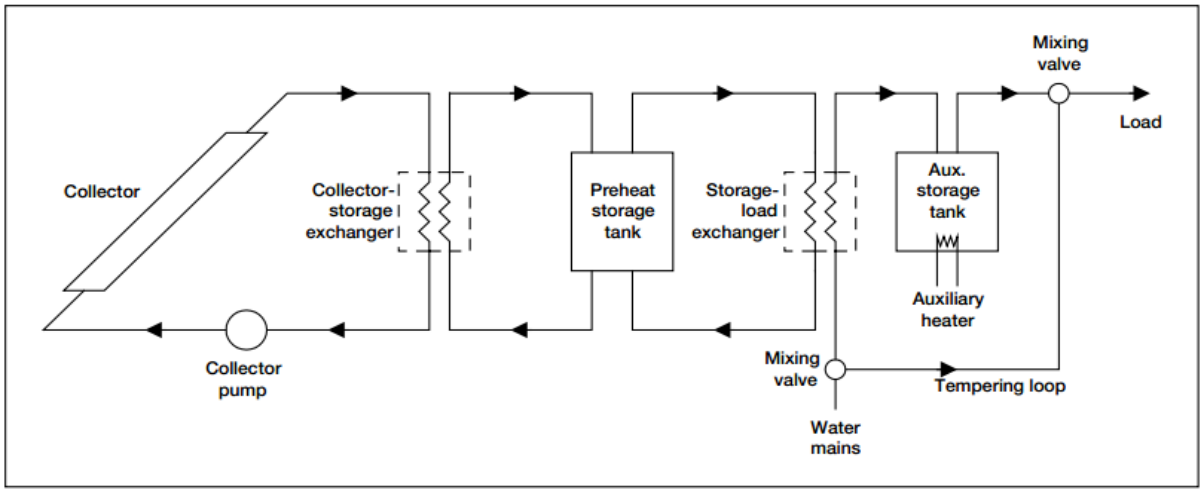

Figure I.11: Diagram of a Solar Domestic Hot Water System.

Where A_c is the solar collector area, F'_Rcollector overall heat removal efficiency correction factor. U_L its collector overall energy loss coefficient, T_{ref} an empirically derived reference temperature (100 °C), $\bar{T}_a$monthly average ambient temperature, L_{tot} monthly total heating load for space heating and hot water. $(\overline{\tau\alpha})$ is the monthly average energy transmittance–absorptance product, $\bar{H}_T$ is the monthly average daily total solar radiation on the collector surface, and N is the number of the day in the month[9].

- $F_R U_L$ and $F'_R(\tau\alpha)_n$are obtained from collector test results, there are two parameters that describe how the collector works[1].
- $F'_R(\tau\alpha)_n$ is an indication of how energy is absorbed and $F_R U_L$ is an indication of how energy is lost. These two parameters constitute the simplest practical collector model.
- The ratio F'_R/F_R corrects for various temperature drops between the collector and the storage tank and is calculated by the equation:

$$\frac{F'_R}{F_R} = \left[1 + \left(\left(\frac{A_C F_R U_L}{(\dot{m}C_P)_c}\right)\left(\frac{(\dot{m}C_P)_c}{\varepsilon(\dot{m}C_P)_{min}} - 1\right)\right)\right]^{-1} \quad \text{(I-12)}$$

Where $(\dot{m}C_P)_{min}$ is the smaller of the fluid capacitance rates (flow rate $\dot{m}$ times fluid heat capacity C_P) on the collector side $(\dot{m}C_P)_c$. The effectiveness ε is given by the equation: $\varepsilon = \frac{Q}{Q_{max}}$.

- The ratios $(\overline{\tau\alpha})/(\tau\alpha)_n$ are obtained from (Appendix: Figure 1) for the beam component at the effective angle of incidence $\bar{\theta}_b$ from (Appendix: Figure 2) and for the diffuse and ground-reflected components at the effective angles of incidence at β from (Appendix: Figure 3).
- The average air temperature $\bar{T}_a$ is obtained from meteorological records for the month and location desired;
- For the monthly loads L calculation, There is no requirement in f-Chart that any particular method be used to estimate the loads;
- Δt is the number of hours in the month: $\Delta t = N \times 24 \times 3600$.

- The total monthly heat demand is sum of the monthly heat user demand and the storage tank loss:

$$L_{tot} = L + Q_s \tag{I-13}$$

where the storage tank losses Q_S for month are given by the relation

$$Q_s = (UA)_S \times \left(\bar{T}_S - T_{s,env}\right) \times \Delta t \tag{I-14}$$

For the temperature in the storage tank $\bar{T}_S$ we have the following equation:

$$\bar{T}_S = \frac{T_{p,min}+T_i}{2} \tag{I-15}$$

5.1.2 f -Chart for liquid systems

For liquid heating systems, the f-chart method is based upon the system configuration shown in Figure I.13. The monthly solar fraction f can be determined from the following relation, which has been obtained by regression from a detailed computer simulation:

$$f = 1.029Y - 0.065X - 0.245\,Y^2 + 0.0018X^2 + 0.0215Y^3 \tag{I-16}$$

This equation cannot be used outside the range shown by the curves in Figure I.13 as a result of its nature. However, if a calculated point falls outside this range, the graph can still be used for extrapolation with satisfactory results. [11].

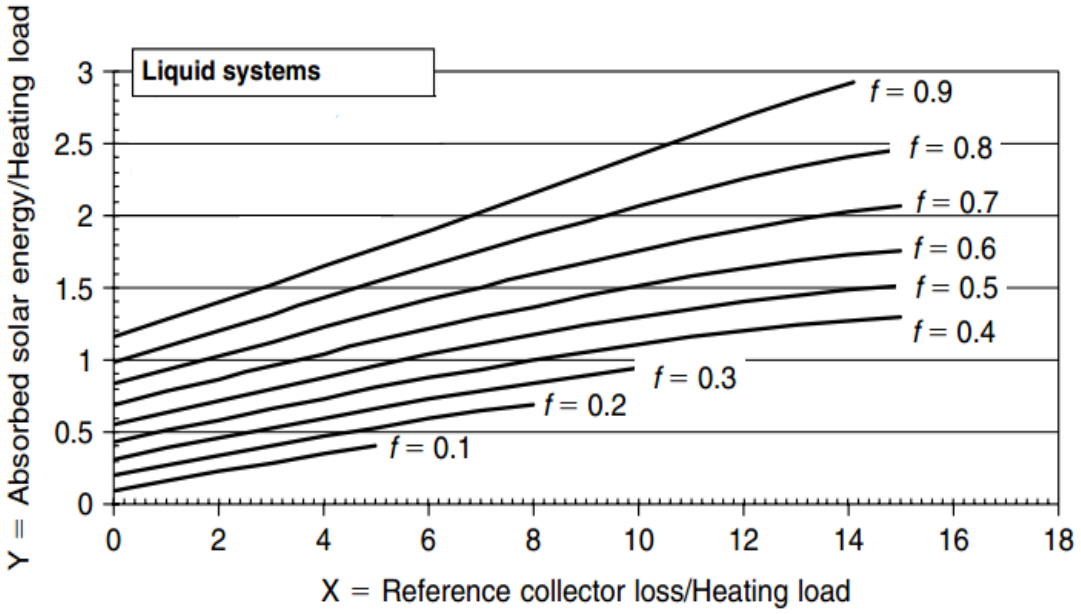

Figure I.12: The f-chart for systems using liquid heat transfer and storage media [2].

For liquid systems, f-chart calculations can be modified to estimate changes in long term performance due to changes in storage tank capacity and load heat exchanger characteristics. This is done by modifying the values of X or Y as described below.

5.1.3 Storage Capacity

The annual performance of a liquid solar system is relatively insensitive to storage capacity as long as the capacity is more than 50 liters of water/square meter of collector [11]. Only small improvements in annual performance can result from any added storage capacity. The f-Chart has been generated for a storage capacity of 75 liters of stored water per square meter of collector area. It can also be used to estimate the annual performance of systems with other storage capacities in the range of 37.5 to 300litre/m² by multiplying the dimensionless parameter X by a storage size correction factor X_c/X (see figure I.14):

$$\frac{X_c}{X}=\left(\frac{actual\ storage\ capacity}{standrad\ storage\ capacity}\right)^{-25} \qquad \text{(I-17)}$$

For $$0.5\leq \left(\frac{actual\ storage\ capacity}{standrad\ storage\ capacity}\right) \leq 4.0$$

Where the standard storage capacity is 75 liters of water per square meter of collector area.

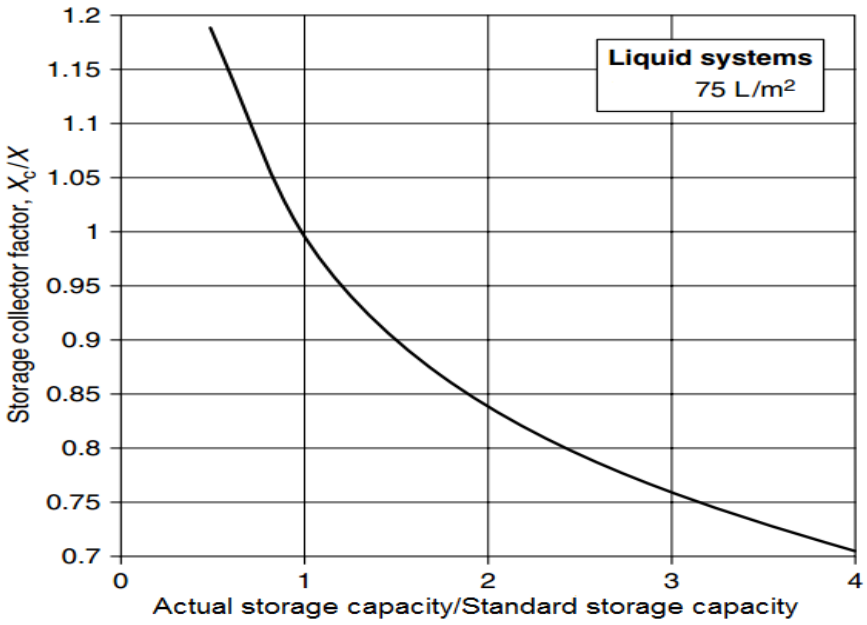

Figure I.13: Storage size correction factor for liquid systems (standard storage size is 75) [2].

5.1.4 Load Heat Exchanger Size

As the heat exchanger used to heat the building air is reduced in size, the storage tank temperature must increase to supply the same amount of heat, resulting in higher collector temperatures and reduced collector output. A measure of the size of the heat exchanger needed for a specific building is provided by the dimensionless parameter $\varepsilon_L C_{min}/(UA)_h$,where ε_L is the effectiveness of the water-air load heat exchanger, C_{min} is the minimum fluid

capacitance rate (mass flow rate times the specific heat of the fluid) in the load heat exchanger and is generally that of the air, and $(UA)_h$ is the overall energy loss coefficient-area product for the building used in the degree-day space heating load model. From thermal considerations, the optimum value of $\varepsilon_L C_{min}/(UA)_h$ is infinity.

However, system performance is asymptotically dependent up on the value of this parameter, and for values of $\varepsilon_L C_{min}/(UA)_h$ greater than 10, performance will be essentially the same as that for the infinitely large value. The reduction in performance due to an undersized load heat exchanger will be significant for values of $\varepsilon_L C_{min}/(UA)_h$ less than about 1. Practical values of $\varepsilon_L C_{min}/(UA)_h$ are generally between 1 and 3 when the cost of the heat exchanger is considered ((Beckman et al. (1977) for further discussion)).

The f-chart for liquid systems was developed with $\varepsilon_L C_{min}/(UA)_h$ = 2. The performance of systems having other values of $\varepsilon_L C_{min}/(UA)_h$ can be estimated from the f-chart by modifying Y by a load heat exchanger correction factor Y_c/Y, as indicated in Equation (I-18) or Figure (15):

$$\frac{Y_C}{Y} = 0.39 + 0.65\exp[-0.139(UA)_h/\varepsilon_L C_{min}] \qquad \text{(I-18)}$$

For $$0.5 \leq \left(\frac{\varepsilon_L C_{min}}{(UA)_h}\right) \leq 50$$

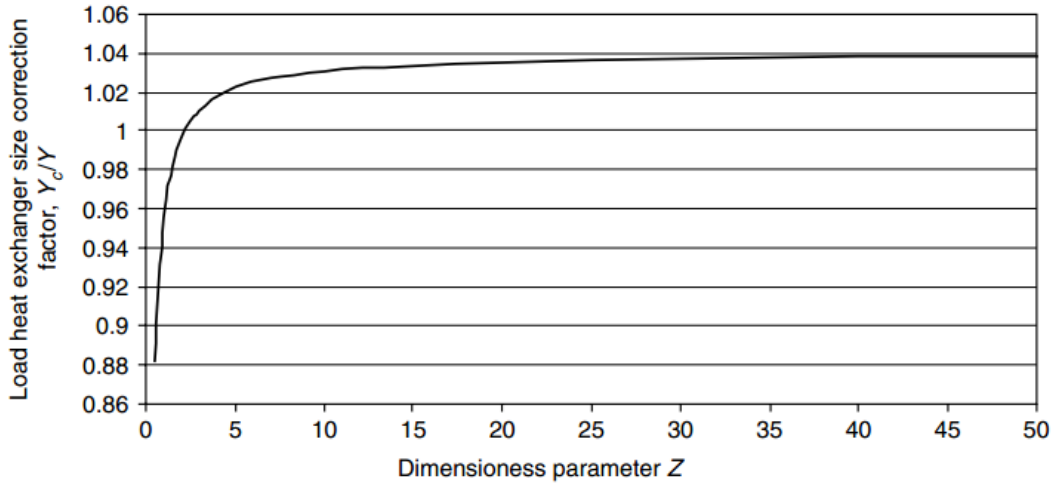

Figure I.14: Load Heat Exchanger Size correction factor [2].

5.2 Utilizability Method

The performance of service water heaters without storage is estimated with the utilizability method. The same method is also used to calculate the energy collected by swimming pool solar collectors. The method enable the calculation of monthly amount of energy delivered by hot water systems without storage, given monthly values of incident solar radiation, ambient temperature and load [10].

5.2.1 Principle of the utilizability method

A solar collector is able to collect energy only if there is sufficient radiation to overcome thermal losses to the ambient. According to equation:

$$\dot{Q}_{capt} = F_R(\tau\alpha)I_T - F_R U_L\,\Delta T \tag{I-19}$$

For a glazed collector this translates into:

$$I_T \geq \frac{F_R U_L (T_i - T_a)}{F_R(\tau\alpha)} \tag{I-20}$$

Where T_i is the temperature of the working fluid entering the collector and all other variables have the same meaning as in equation (I-19). This makes it possible to define a critical irradiance level I_C which must be exceeded in order for solar energy collection to occur. Since the model is dealing with monthly averaged values, I_C is defined using monthly average transmittance-absorptance ($\overline{\tau\alpha}$) and monthly average daytime temperature during the hours of sunning $\bar{T}_a$ (assumed to be equal to the average temperature plus 5°C) through:

$$I_C \geq \frac{F_R U_L (T_i - \bar{T}_a)}{F_R(\overline{\tau\alpha})} \tag{I-21}$$

Combining this definition with equation (I-19) leads to the following expression for the average daily energy Q collected during a given month:

$$Q = \frac{1}{N} + \sum_{joures}\sum_{heures} A_c F_R(\overline{\tau\alpha})\,(I_T - I_C)^+ \tag{I-22}$$

Where N is the number of days in the month, $\boldsymbol{I_T}$ is the hourly irradiance in the plane of the collector, and the + superscript denotes that only positive values of the quantity between brackets are considered.

The monthly average daily utilizability $\overline{\Phi}$, is defined as the sum for a month, over all hours and days, of the radiation incident upon the collector that is above the critical level, divided by the monthly radiation:

$$\overline{\Phi} = \frac{\sum_{jours}\sum_{heures}(I_T - I_C)^+}{\bar{H}_T N} \tag{I-23}$$

Where $\bar{H}_T$ is the monthly average daily irradiance in the plane of the collector. Substituting this definition into equation (I-22) leads to a simple formula for the monthly useful energy gain:

$$Q = A_c\, F_R(\overline{\tau\alpha})\, \bar{H}_T \overline{\Phi} \tag{I-24}$$

The purpose of the utilizability method is to calculate Φ from the collector orientation and the monthly radiation data entered by the user. The method correlates Φ to the monthly average clearness index $\bar{K}_T$ and two variables: a geometric factor $\bar{R}/R_n$ and a dimensionless critical radiation level $\overline{X}_c$, as described hereafter.

5.2.2 Geometric factor $\bar{R}/R_n$:

$\bar{R}$ is the monthly ratio of radiation in the plane of the collector, $\bar{H}_T$, to that on a horizontal surface, $\bar{H}$:

$$\bar{R} = \frac{\bar{H}_T}{\bar{H}} \tag{I-25}$$

Where $\bar{H}_T$ is calculated by the equation (I-8), R_n is the ratio for the hour centered at noon of radiation on the tilted surface to that on a horizontal surface for an average day of the month. This is expressed through the following equation:

$$R_n = \left(1 - \frac{r_{d,n}\, H_d}{r_{t,n}\, H}\right) R_{b,n} + \left(\frac{r_{d,n}\, H_d}{r_{t,n}\, H}\right) \left(\frac{1+cos\beta}{2}\right) + \rho_g \left(\frac{1-cos\beta}{2}\right) \tag{I-26}$$

Where $r_{d,n}$ is the ratio of hourly total to daily total radiation, for the hour centered around solar noon. $r_{t,n}$, is the ratio of hourly diffuse to daily diffuse radiation, also for the hour centered around solar noon. This formula is computed for an "average day of month," i.e. a day with daily global radiation H equal to the monthly average daily global radiation $\bar{H}$; H_d is the monthly average daily diffuse radiation for that "average day".

$r_{t,n}$ is computed by the Collares-Pereira and Rabl equation [1], written for solar noon:

$$r_{t,n} = \frac{\pi}{24}(a+b)\frac{1-cos\omega_S}{sin\,\omega_S - \omega_S\, cos\omega_S} \tag{I-27}$$

$$a = 0{,}409 + 0{,}5016\, sin\left(\omega_s - \frac{\pi}{3}\right) \tag{I-28}$$

$$b = 0{,}6609 - 0{,}4767\, sin\left(\omega_s - \frac{\pi}{3}\right) \tag{I-29}$$

$r_{d,n}$, is computed by the Liu and Jordan equation, written for solar noon:

$$r_{d,n} = \frac{\pi}{24}\frac{1-cos\omega_S}{sin\omega_S - \omega_S cos\omega_S} \tag{I-30}$$

5.2.3 Dimensionless critical radiation level $\bar{X}_c$

$\bar{X}_c$ is defined as the ratio of the critical radiation level to the noon radiation level on the typical day of the month:

$$\bar{X}_C = \frac{I_c}{r_{t,n} R_n \bar{H}} \tag{I-31}$$

5.2.4 Monthly average daily utilizability $\bar{\Phi}$

Finally, the correlation giving the monthly average daily utilizability $\bar{\Phi}$, as a function of the two factors $\bar{R}/R_n$ and $\bar{X}_c$ calculated previously is:

$$\bar{\Phi}(\bar{X}_C) = exp\left\{\left[a + b\,\frac{R_n}{\bar{R}}\right][\bar{X}_c + c\bar{X}_c^2]\right\} \quad \text{(I-32)}$$

With:

$a = 2{,}943 - 9{,}271\,\bar{K}_T + 4{,}031\,\bar{K}_T^2$
$b = -4{,}345 + 8{,}853\,\bar{K}_T - 3{,}602\,\bar{K}_T^2$
$c = -0{,}170 - 0{,}306\,\bar{K}_T + 2{,}936\,\bar{K}_T^2$

The amount of energy collected can be computed, as shown earlier in equation (I-24) [10].

5.3 The $\bar{\Phi}$, f -chart method

Now we will see how Klein and Beckman (1979) have combined the potential for daily utilizability with the concept of f-Chart to explain the finite storage capacity (the $\bar{\Phi}$,, the f-chart method). In each case we will see how critical levels of radiation are established and illustrate the use of methods.

Design methods are available for many solar-thermal systems, but not all. All utilizability methods require knowledge of the temperature of liquid at the collector input, which often unknown. The $\bar{\Phi}, f$-chart method is a combination of the utilizability method and f-chart methods, applied in systems where the energy supplied to load is above a minimum useful temperature and the temperature of this energy supply has no effect on the performance of the load system as long as it is greater than the minimum temperature.

The utilizability design concept is useful whenever the collector operates at a known critical radiation level throughout a month. In a more typical situation, the collector is connected to a tank so that the monthly sequence of weather and the load time distribution result in a fluctuating storage tank temperature and consequently a variable critical radiation level.

In these solar systems, the thermal energy delivered to the heating load must heat the water at a temperature having a value greater than that called minimum temperature specified by the user. Consequently, the maximum monthly average daily energy that can be delivered from the system shown in figure I.16 is given by:

$$\sum \bar{Q}_{u,max} = A_c F_R\,(\overline{\tau\alpha})\bar{H}_T\,\bar{\Phi}_{max} \quad \text{(I-33)}$$

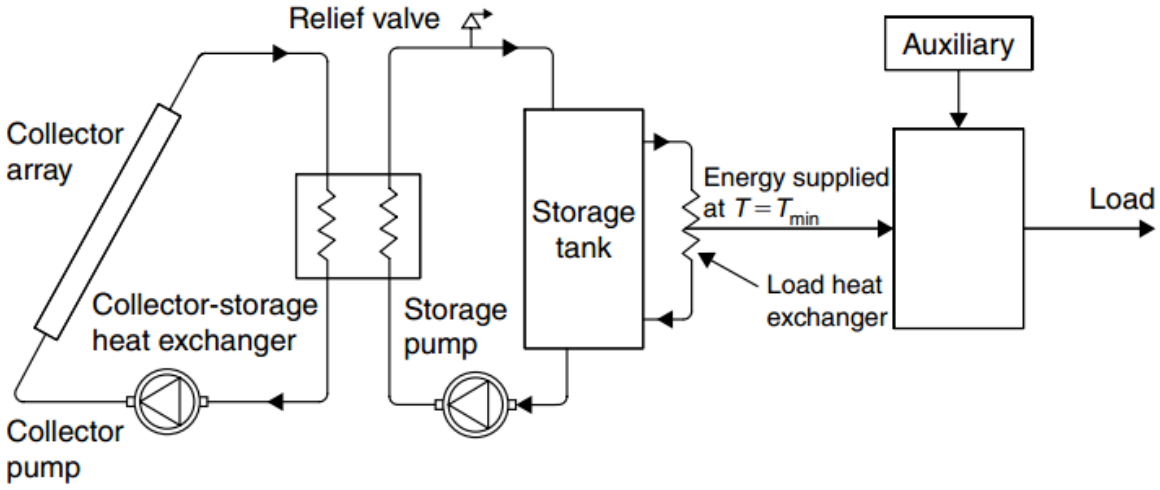

Figure I.15: Energy solar system (closed-loop) [2].

This is the same equation as (I-33) except that $\overline{\Phi}$ is replaced with $\overline{\Phi}_{max}$, which is the maximum daily utilizability, estimated from the minimum monthly average critical radiation ratio:

$$\bar{X}_{c,min} = \frac{\frac{F_R U_L \left(T_{p,min} - \bar{T}a\right)}{F_R(\overline{\tau\alpha})}}{r_n R_n \bar{K}_T \bar{H}_0} \tag{I-34}$$

To combine the two concepts, Klein et al. modified and replaced the expressions of X and Y variables used in the f-chart method by those given as follows:

The ordinate Y is replaced by:

$$\overline{\Phi}_{max} Y = \overline{\Phi}_{max} \frac{A_c F_R(\overline{\tau\alpha}) \bar{H}_T N}{L_{tot}} \tag{I-35}$$

And the abscissa is replaced by the modified value X ':

$$\boldsymbol{X' = \frac{A_c F_R U_L (100)\, \Delta t}{L\_tot}} \tag{I-36}$$

So, the correlation expressed by the thermal load of the covered by the solar system is given by the following equation:

$$f_{tl} = \overline{\Phi}_{max} Y - 0.015(e^{3.85f} - 1)(1 - e^{3.85X'})(R_s)^{0.76} \tag{I-37}$$

Where:

R_s is the ratio of the standard storage heat capacity per unit of collector area of (350 kJ/m² C) to the actual storage capacity, given by:

$$R_s = \frac{350}{\frac{MC_P}{A_C}} \quad \text{(I-38)}$$

Although f is given implicitly by Equation (I-33), it is easy to solve for f by Newton's method or by trial and error [9]. Since the $\bar{\Phi}, f$-charts are given for various storage capacities and the user has to interpolate, the use of Equation (I-33) is preferred. The $\bar{\Phi}, f$-charts are used in the same way as f-chart meth. The values of $\bar{\Phi}_{max}Y$, and X' need to be calculated from the long-term radiation data for the particular location and load patterns.

The average daily utilizability is given from the formula

$$\bar{\Phi} = \frac{f_{tl}}{Y} \quad \text{(I-39)}$$

Where $\bar{\Phi}$ relates $\bar{\Phi}_{max}$ by the relation:

$$\bar{\Phi}_{max}=\bar{\Phi}\left(\bar{X}_{c,min}\right) \quad \text{(I-40)}$$

The heat exchanger adds a resistive between the storage tank and the load. Doing so, it reduces the useful energy and increase storage tank losses. This can be modeled by the following formula:

$$T_{p,min} - T_{min} = \frac{fL/\Delta t_h}{\varepsilon_L \, C_{min}} \quad \text{(I-41)}$$

The solar fraction f can be related to the total fraction of the monthly load supplied by solar energy f_{tl} and to the useful load by the relation:

$$f = f_{tl} \times \left(1 + \frac{Q_s}{L}\right) - \frac{Q_s}{L} \quad \text{(I-42)}$$

6. Conclusion

The heat produced by a thermal solar installation makes it possible to provide directly for needs, contrary to a photovoltaic solar installation which its electrical production is entirely injected on the electrical communication. The dimensioning of a thermal solar system and the determination of an optimal collecting area, has become a primary concern in the design of solar systems to meet the hot water needs, building heating the industry heating. Indeed, the influence of designing compared to the reliability of the results of a heating sanitary water is very important.

Chapter II: Results and Discussion

1. Introduction

A numerical modeling of the solar thermal System is a set of mathematical equations to solve physical problems by appropriate simplification of reality. In this second chapter we show how to implement the φ-f chart method with Scilab. This model can be used to calculate the solar fraction for hot water production with respect to the global request. This Scilab code can be used to estimate the thermal performance of solar energy systems for domestic water, industrial process heating, and space heating systems where the thermodynamics cycle efficiency is independent of the heat supply temperature. We also integrated a mathematical model for the determination of optimal collector area of the solar installations for collective water heating. This method is based on a minimization of the total cost of the installation. This by holding account, not only costs of the various components and price of the conventional energy consumed by the auxiliary system, but also of the thermal performances of the installation starting from the φ-f chart method.

2. Solar thermal system modeling

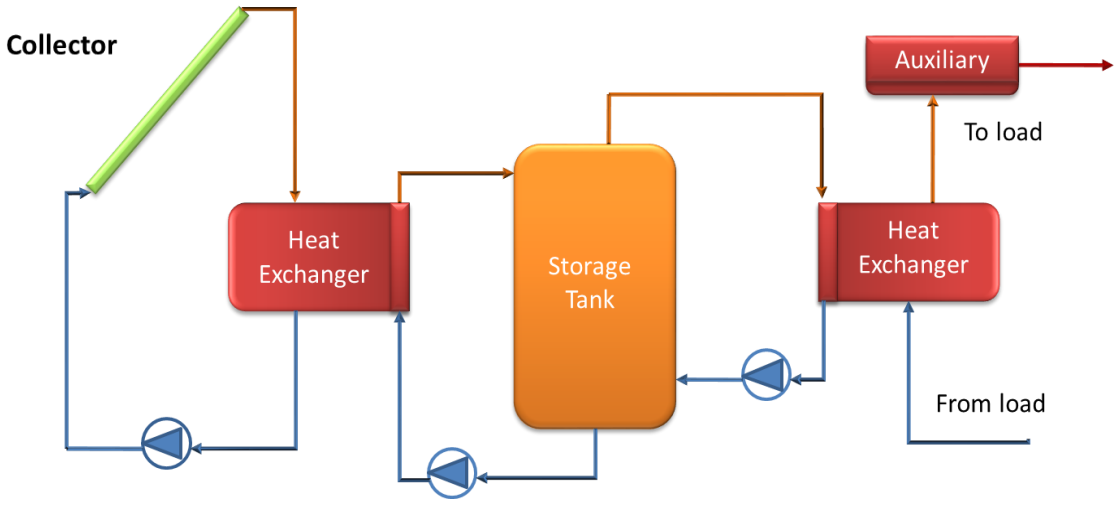

Figure II.1: Schematic diagram of a closed loop solar energy system.

2.1 Program algorithm

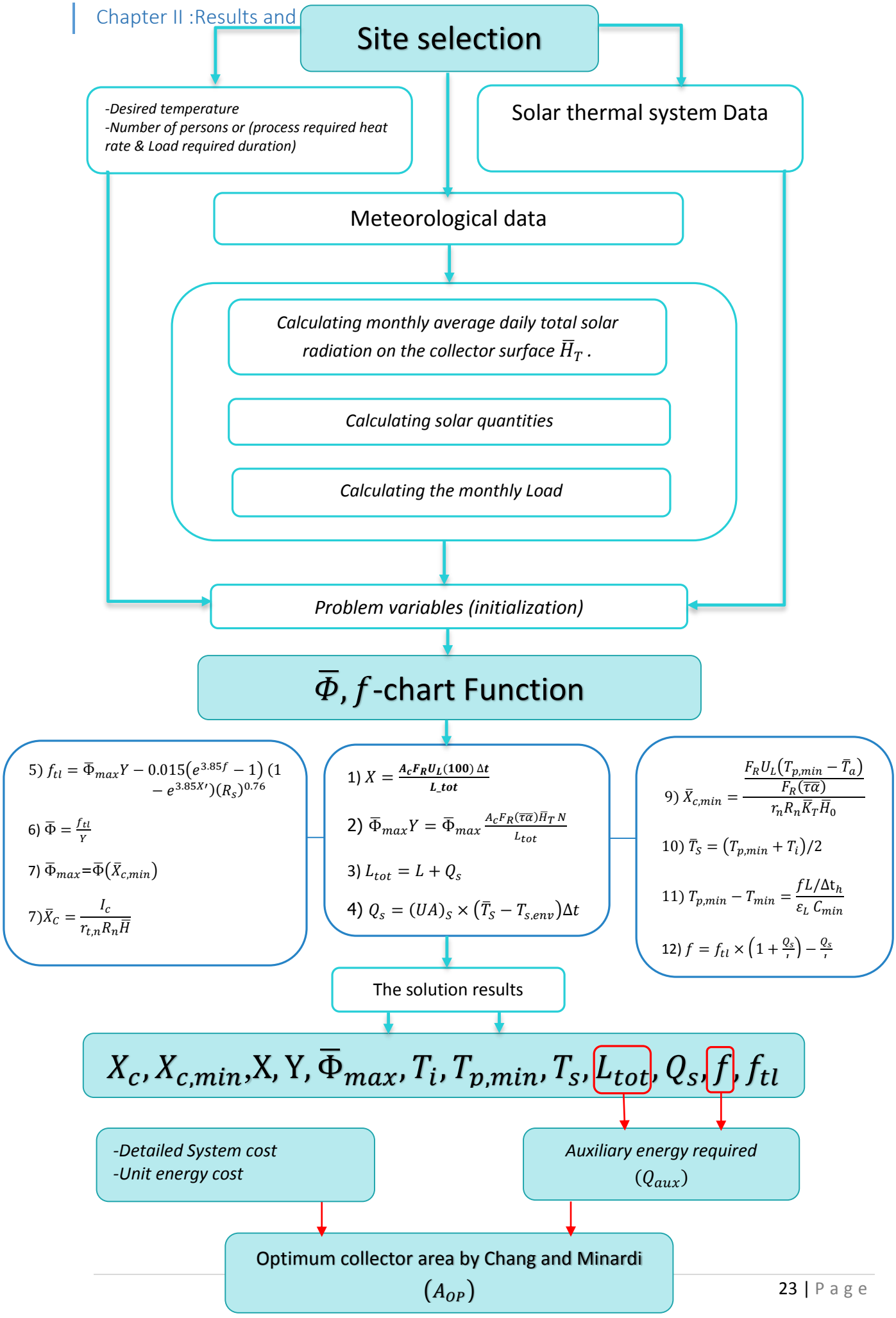
Site selection
-Desired temperature
-Number of persons or (process required heat rate & Load required duration)
Solar thermal system Data
Meteorological data
Calculating monthly average daily total solar radiation on the collector surface $\bar{H}_T$.
Calculating solar quantities
Calculating the monthly Load
Problem variables (initialization)
$\bar{\Phi}, f$-chart Function
5) $f_{tl} = \bar{\Phi}_{max} Y - 0.015(e^{3.85f} - 1)(1 - e^{3.85X'})(R_s)^{0.76}$
6) $\bar{\Phi} = \frac{f_{tl}}{Y}$
7) $\bar{\Phi}_{max} = \bar{\Phi}(\bar{X}_{c,min})$
7) $\bar{X}_C = \frac{I_c}{r_{t,n} R_n \bar{H}}$
1) $X = \frac{A_c F_R U_L (100)\,\Delta t}{L\_tot}$
2) $\bar{\Phi}_{max} Y = \bar{\Phi}_{max} \frac{A_c F_R (\bar{\tau}\bar{\alpha}) \bar{H}_T N}{L_{tot}}$
3) $L_{tot} = L + Q_s$
4) $Q_s = (UA)_S \times (\bar{T}_S - T_{s,env})\Delta t$
9) $\bar{X}_{c,min} = \frac{\frac{F_R U_L (T_{p,min} - \bar{T}_a)}{F_R(\bar{\tau}\bar{\alpha})}}{r_n R_n \bar{K}_T \bar{H}_0}$
10) $\bar{T}_S = (T_{p,min} + T_i)/2$
11) $T_{p,min} - T_{min} = \frac{fL/\Delta t_h}{\varepsilon_L C_{min}}$
12) $f = f_{tl} \times \left(1 + \frac{Q_s}{r}\right) - \frac{Q_s}{r}$
The solution results
$X_c, X_{c,min}$,X, Y, $\bar{\Phi}_{max}, T_i, T_{p,min}, T_s, L_{tot}, Q_s, f, f_{tl}$
-Detailed System cost
-Unit energy cost
Auxiliary energy required (Q_{aux})
Optimum collector area by Chang and Minardi (A_{OP})

2.2 Scilab Softwre

Scilab is a freely distributed open source scientific software package, first developed by researchers from INRIA and ENPC, and now by the Scilab Consortium. It is similar to Matlab, which is a commercial product. Yet it is almost as powerful as Matlab. Scilab consists of three main components:

- an interpreter
- libraries of functions (Scilab procedures)
- libraries of Fortran and C routines

Scilab is specialized in handling matrices (basic matrix manipulation, concatenation, transpose, inverse, etc.) and numerical computations. Also it has an open programming environment that allows users to create their own functions and libraries [18].

The formulation of the system of equations yields to a nonlinear system of 12 equations in 12 unknowns that is solved in Scilab using the function "fsolve".

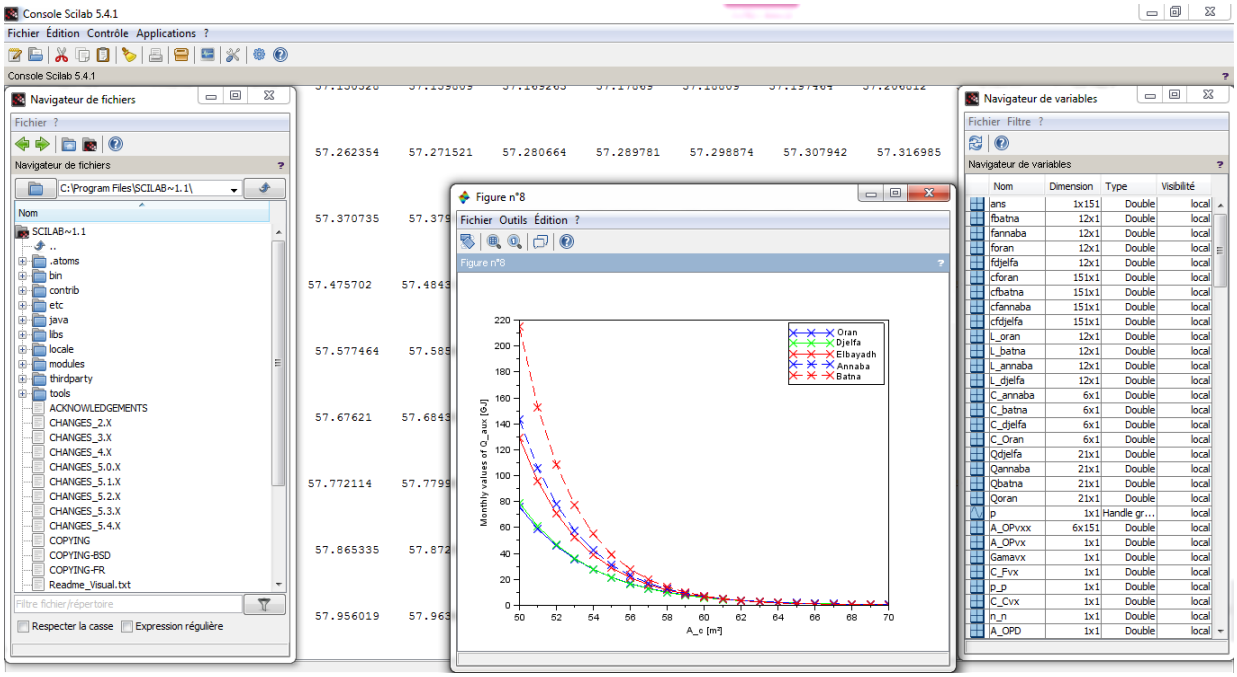

Figure II.2: Scilab interface.

2.3 Load calculation

2.3.1 Hot water demand

It is the water mass received from the public network, which should be heated at a fixed temperature according to the needs and which is generally equal to 55 degrees in the case of a residential system of water service. With the absence of precise data, and according to the lifestyle of the North and that of the South of our country, thus differ the requirements

out of hot water, and also differ from a site to another. For our case, the request M_{hw} as regards hot water mass is calculated by the relation presented in [9], given as:

$$M_{hw} = \left(\frac{25}{\left(1+\left(\frac{10}{(40-T_N)}\right)\right)}\right) + \left(\frac{15}{1+\left(\frac{18}{32-T_N}\right)}\right) + \left(\frac{21.5}{1+\left(\frac{13}{37-T_N}\right)}\right) + \left(\frac{7}{1-\left(\frac{15}{65-T_N}\right)}\right) + \left(\frac{8}{1+\left(\frac{10}{45-T_N}\right)}\right) \quad \text{(II.1)}$$

2.3.2 Cold water temperature

Temperature of the cold water supplied by the public water system is used to calculate the energy needed to heat water up to the desired temperature. In our case we used the method presented in [9] to calculate cold water temperature**,** it is computed from minimum and maximum values specified by the user.

A sinusoidal profile is generated from the minimum and maximum temperatures specified by the user, assuming the minimum is reached in February and the maximum in August in the Northern Hemisphere (the situation being reversed in the Southern Hemisphere). Hence the average soil (or cold water) temperature T_N is expressed as a function of minimum temperature T_{min}, maximum temperature T_{max}, and month number *n* as:

$$T_N = \frac{T_{min}+T_{max}}{2} - \frac{T_{max}-T_{min}}{2}\, h\, cos\left(2\pi\, \frac{n-2}{12}\right) \quad \text{(II.2)}$$

Where *h* is equal to 1 in the Northern Hemisphere and –1 in the Southern Hemi-sphere.

The thermal load is calculated by the following equation:

$$L = M_{hw} \times (T_{des} + T_N) \times N_P \quad \text{(II.3)}$$

3. Applications

3.1 Application for residential building

Solar water heating system for residential building has a 65 m² collector. The system is located in Djelfa (34° 40′ 00″ N latitude), and the collector characteristics are: $F_R U_L = 4.5\ W/m^{2\circ}C$, $F_R\ (\tau\alpha\ )_n = 0.85, F'_R/F_R = 0.95$, tilted at 31° (south orientation). The heat exchanger has effectiveness $\varepsilon_L = 0.75$, $C_{min} = 5000\ WK^{-1}$, The persons number is 35 and the desired temperature is 55 °C.

3.1.1 Conception results:

Figure II.3 shows how great decrease in demand for hot water during the summer. It is evident that increasing the ambient temperature, the load values decreases (inverse proportion).

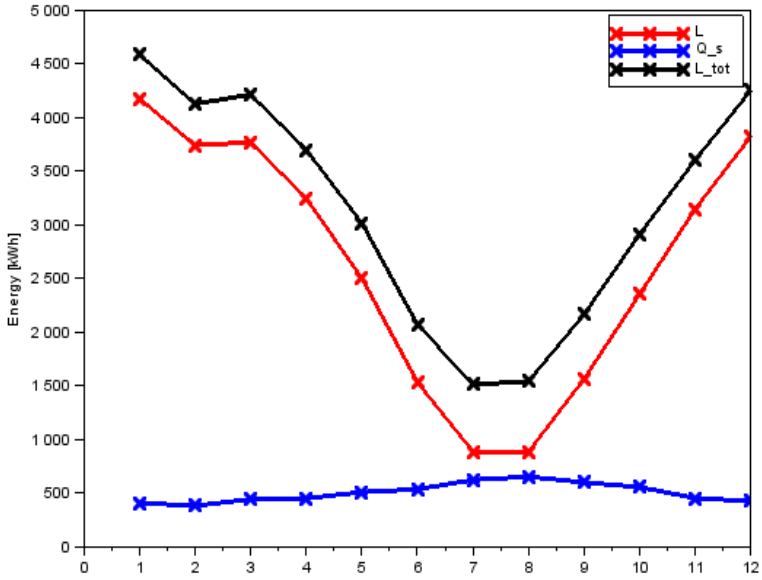

Figure II.3: Numerical results during the 12 months for L,Q_S, L_{tot}.

Figure II.3 shows the monthly variation of: the inlet collector fluid temperature, useful energy temperature, monthly average storage tank temperature, where the ambient temperature affects the rest of the temperatures mentioned.

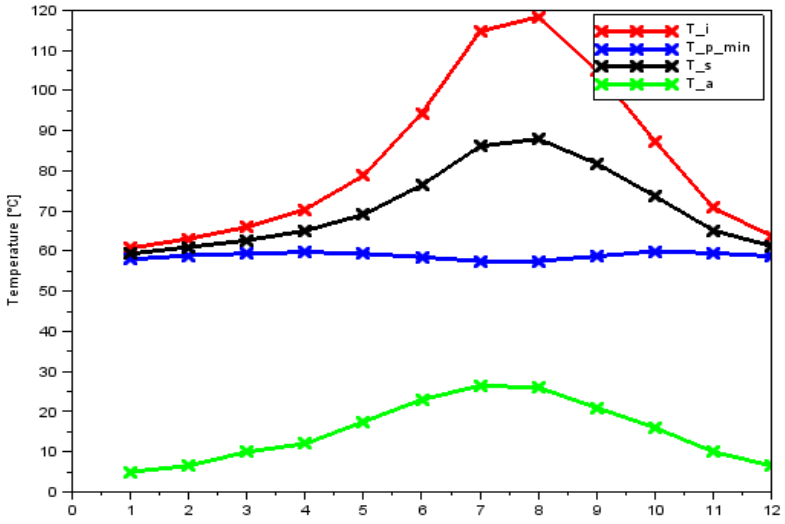

Figure II.4: Numerical results during the 12 months for $T_i, T_{p,min}, T_s, T_a$.

The figure II.5 describe the monthly performances of the solar thermal system. The variations are directly effects by the collector area, the monthly load and the ambient temperature, which are due to the incident solar radiation, and because the area is already fixed and the load goes proportionally with the ambient temperature, so it will have the same behavior with the solar fraction variations. We can notice that the highest fraction is reached in July and August.

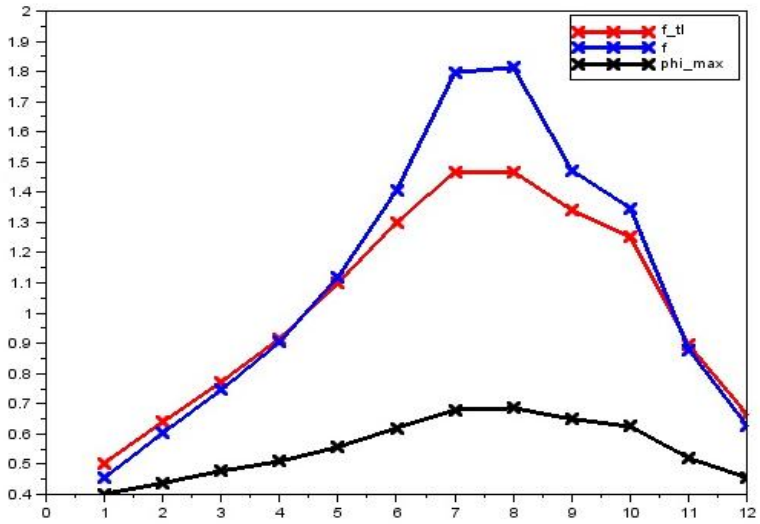

Figure II.5: Numerical results during the 12 months of for $f, f_{tl}, \overline{\Phi}_{max}$.

In figure II.6 we can see the variation of the two dimensionless parameters X which represents the energy losses, Y which represents the energy gain of the collector, $\bar{X}_c$ dimensionless average daily critical level of the solar collector, $\bar{X}_{c,min}$ minimum of the dimensionless average daily critical level of the solar collector , all the variation are related to the incident solar radiation.

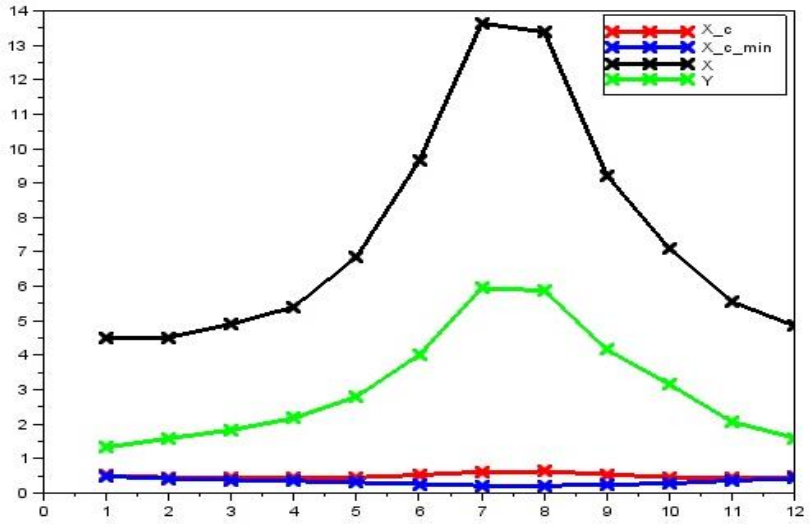

Figure II.6: Numerical results during the 12 months for X, Y, $X_c, X_{c,min}$.

Figure II.7 shows the monthly average daily total solar radiation on a horizontal surface for Djelfa city, the measurement of monthly average daily extraterrestrial solar radiation and clearness index shows (see equation I-7) that the maximum monthly radiation in Djelfa is reached in July.

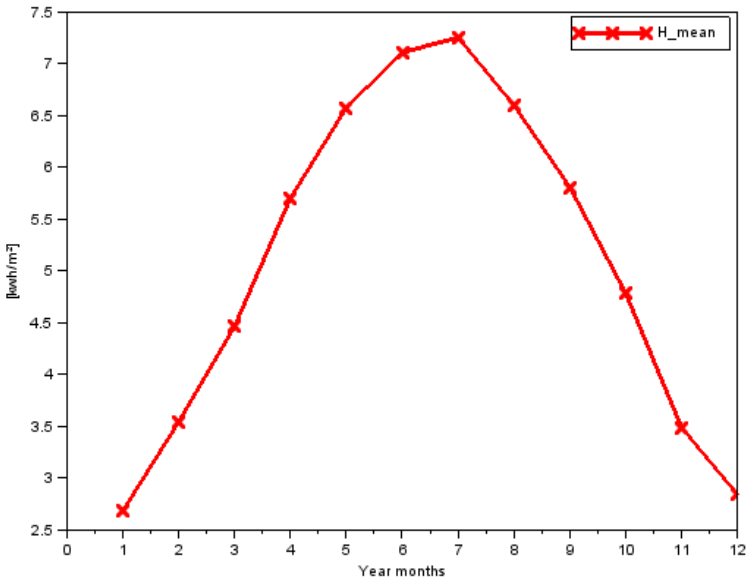

Figure II.7: Numerical results during the 12 months for $\overline{H}_T$.

3.1.2 Varying the parameters:

In this section we provide some results about parameters variation. The previous application is here simulated by varying one parameter at once. The following figures report the solar fraction for hot water production during the year.

Figure II.8 shows the solar fraction during the year for three different collecting areas: 60m², 65m² and 70 m². It is evident that increasing the collecting area, the faction increases. Moreover we may notice that the highest fraction in Djelfa is reached in July and August. This is due to the maximum value of the incident solar radiation.

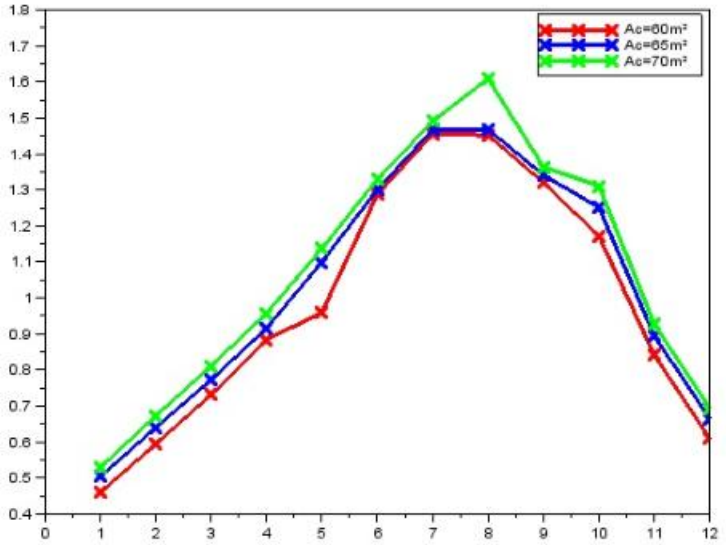

Figure II.8: Solar fraction with different collecting areas.

Figure II.9 describes the behavior of the solar fraction during the year for two different number of persons need hot water: 31, and 35. It is visible that less number of persons which mean lower demand of hot water all over the year.

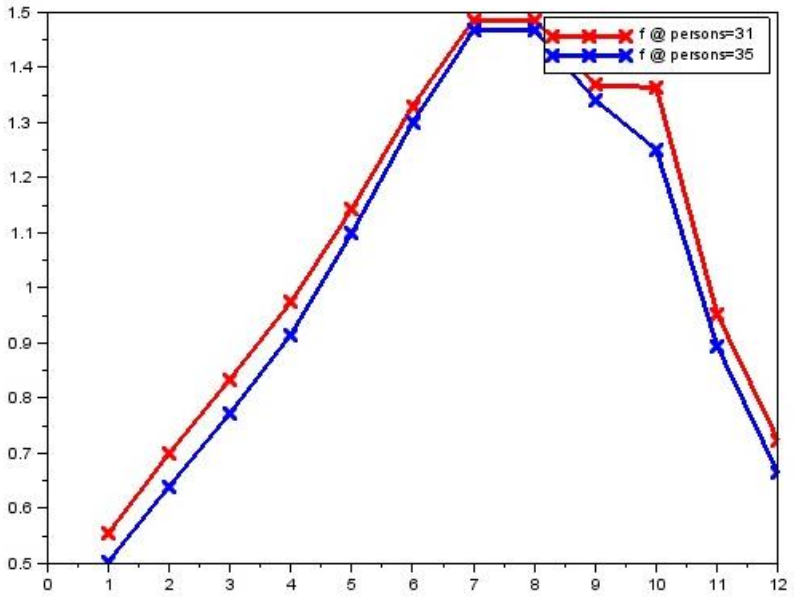

Figure II.9: Solar fraction with different number of persons.

Figure II.10 contains the last set of experiments that have been carried out by changing the minimum required temperature. The experiments have been done for three different values: 50°C, 55°C and 60°C. The effect is simple all year round, the less the requirement, the higher the solar fraction.

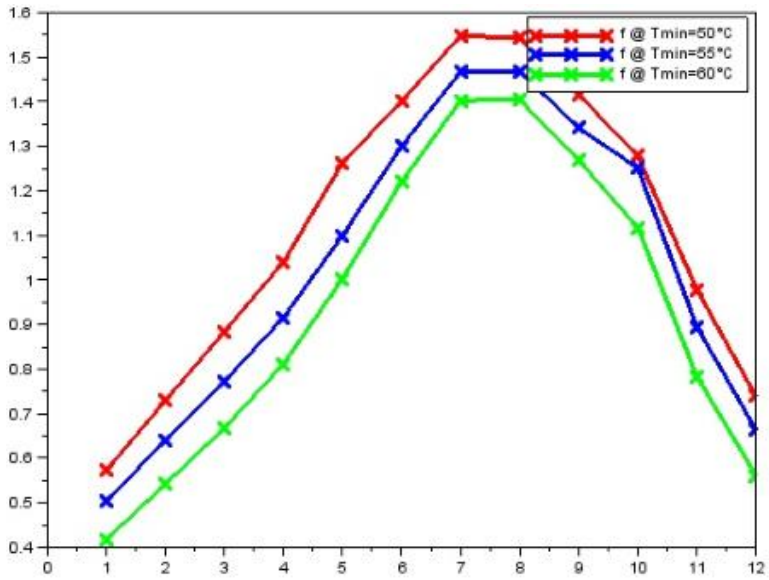

Figure II.10: Solar fraction with different minimum temperature requirements.

Figure II.11 shows the solar fraction during the year for five different locations: Djelfa, Elbayadh, Oran, Batna and Annaba. The increases is related to the variation of hot

water demand and ambient temperature as shown in figure II.3. We can see that the highest fraction in all the sites shown is reached in July and August. This is due to the maximum value of the incident solar radiation.

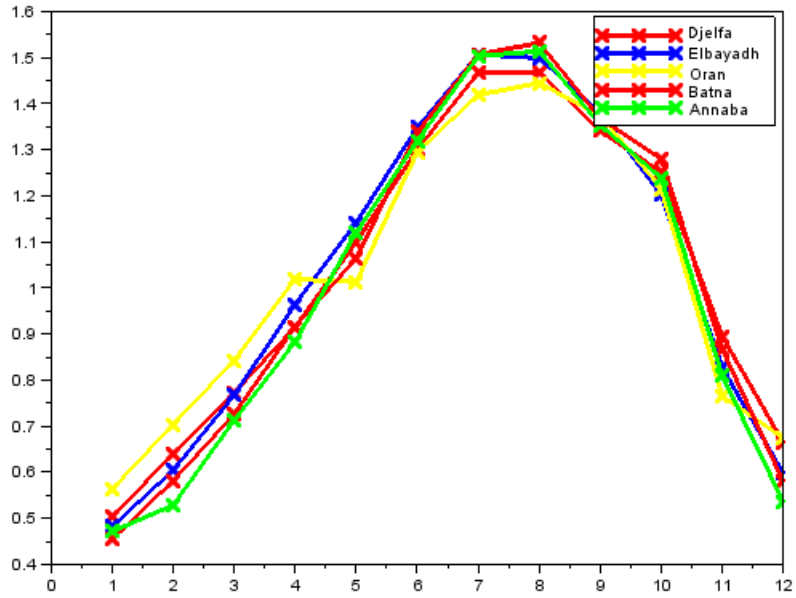

Figure II.11: Solar fraction monthly variation with different locations (Wilaya).

Figure II.12 shows that there is a great decrease in demand for hot water during summer for all the five sites: Djelfa, Oran, Elbayadh, Batna and Annaba. It is evident that increasing the ambient temperature, the load values decreases (inverse proportion).

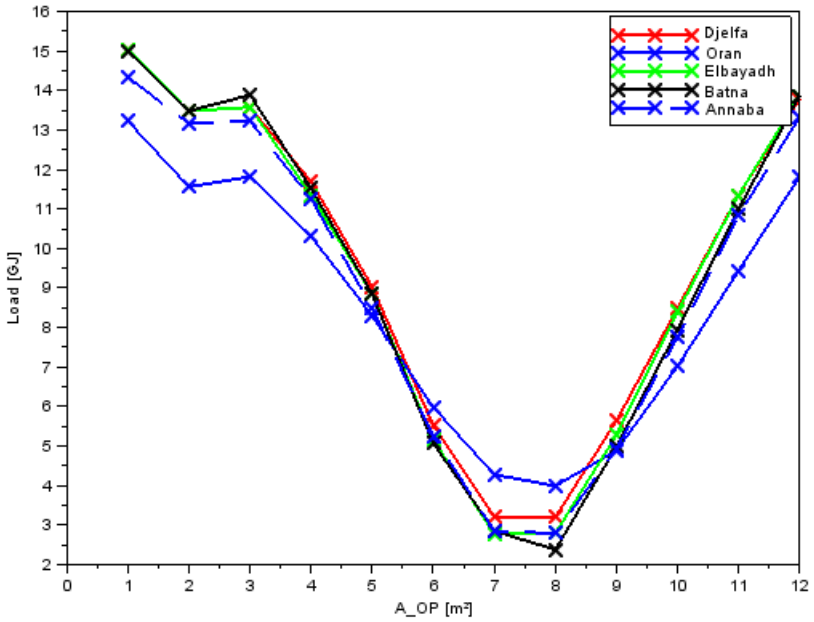

Figure II.12: Load estimated for different locations (same parameters).

3.2 An Optimization Formulation for Solar Heating Systems

The most important concern in the design of solar heating systems is the optimal solar collector area which is defined as the area that optimizes the system from both economic and parametric viewpoints. This area is the result of a cost- benefit approach. The cost of the solar system and benefits of saving of the cost of auxiliary fuel accruing from the installation of the system.

3.2.1 Chang and Mirandi approch

The method described below is used to calculate the minimum total cost of a solar water heater composed by the following systems: a collection system, a system of storage and backup system.

Annual operating cost is generally expressed as [17]:

$$C_{\text{TOTAL}} = (C_C A_C + C_T b A_C + C_\gamma A_C) I + Q_{aux} c_F + M \quad \text{(II.4)}$$

$$I = \frac{i(1+i)^n}{[(1+i)^n - 1)]} \quad \text{(II.5)}$$

Where:

- Q_{aux} the annual auxiliary (back up) energy consumption;
- c_F the unit of electricity cost (DA/kWh);
- c_c the cost of solar collector panel per unit area (DA/m^2);
- C_T the storage tank cost per unit volume (DA/m^3);
- C_γ the other collector directly related costs (DA/m^2);
- M the cost independent of collector areas (DA);
- i= the annual interest rate.
- n the number of payment years.
- The volume of the tank was assumed to vary directly with the collector area with the proportionality constant b (m^{-2}).

The optimum surface can be determined by solving the following equation:

$$\frac{dC_{TOTAL}}{dA_C} = 0 \quad \text{(II.6)}$$

3.2.2 Determination of the collector surface

Energy of the auxiliary system is given by the following expression:

$$Q_{aux} = (1 - f)L \quad \text{(II.7)}$$

To find a relationship between the energy consumed by the auxiliary system (Q_{aux}) and the capture area, next figure shows an example requirement for auxiliary energy from the previous application (Djelfa):

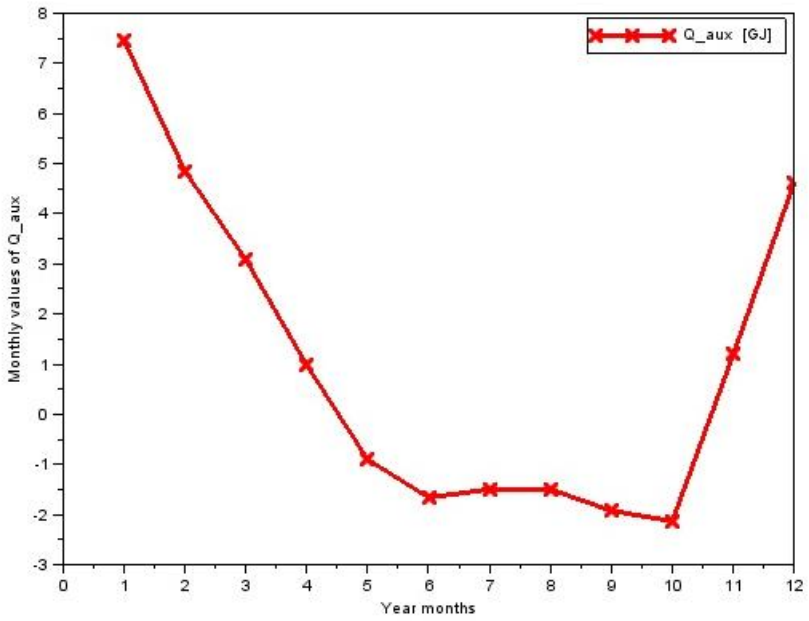

Figure II.13: Monthly variation of auxiliary energy required for Djelfa case.

Chang and Minardi have calculated the solar fraction f for different surfaces capture. The graphical representation of Q_{aux} shows it changes according to a law close to an exponential law:

$$Q_{aux} = Q_m exp(-\lambda A_C) \quad \text{(II.8)}$$

The parameters λ and Q_m are the characteristics of the auxiliary system, determined by location and system characteristics for giving operating conditions.

Then, Chang and Minardi [17] have shown that, by inserting equation (II.4)in equation (II.8)and differentiating with respect to A_C, the optimal collector area, A_{op}, is given by:

$$A_{OP} = \frac{1}{\lambda} ln \left[\frac{Q_m C_F \lambda}{(C_C + bC_T + C_\gamma) I} \right] \quad \text{(II.9)}$$

Where:

A_{OP} is the optimum collector area.

Equation (II.9) provides a rapid method of obtaining A_{OP}. Both system parameters and economic factors affect the value of A_{OP}. This equation indicates that A_{OP} increases if fuel cost increases, load increases, system cost decreases and Q_{aux} decay constant decreases.

For convenience, equation (II.9) can be rewritten as:

$$A_{OP}=\frac{1}{\lambda}\ln\gamma \quad \text{(II.10)}$$

Where

$$\gamma=\frac{Q_m C_F \lambda}{(C_C+bC_T+C_\gamma)I} \quad \text{(II.11)}$$

The parameter γ, reflects a saving to cost ratio. Economic feasibility of a solar system exists only if $\gamma \geq 1$.

An example of results is given in figure II.14, for T_{min}=55C° to heat water for 35 person.

We plotted the annual auxiliary energy according the collecting area, for different Wilaya for the same number of people and the same desired temperature, the results are given by following figure.

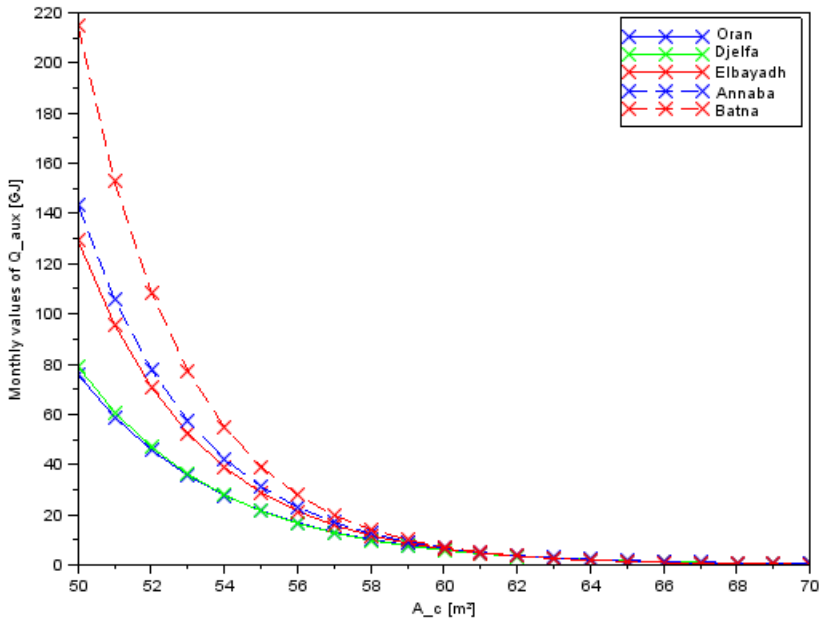

Figure II.14: Auxiliary energy required vs. collector area with different Wilaya.

Figure II.15 shows the optimal area variation vs the collector cost (1m²). The formula (II.9) have been used for different Wilaya in Algeria: Oran, Elbayadh, Djelfa, Batna and Annaba, we may notice the high cost of the collector effect on the optimal area, the results means that as much as the collector cost keep rising as much as it is advisable to compensate the energy obtained from the difference area between the optimal and the proposed one by the auxiliary energy to get the best economic benefit.

- With

  - c_F=4.179 DA/kWh
  - C_T DA/m^3
  - C_γ 4000DA/m^2
  - i=0.11 [16]
  - c_c 30,000 DA/m^2 [15]
  - M 50,000 DA
  - $n = 20\ Year$
  - $b = 0.06\ m^{-2}$ [17]

The optimum surface can be determined by solving the following equation:

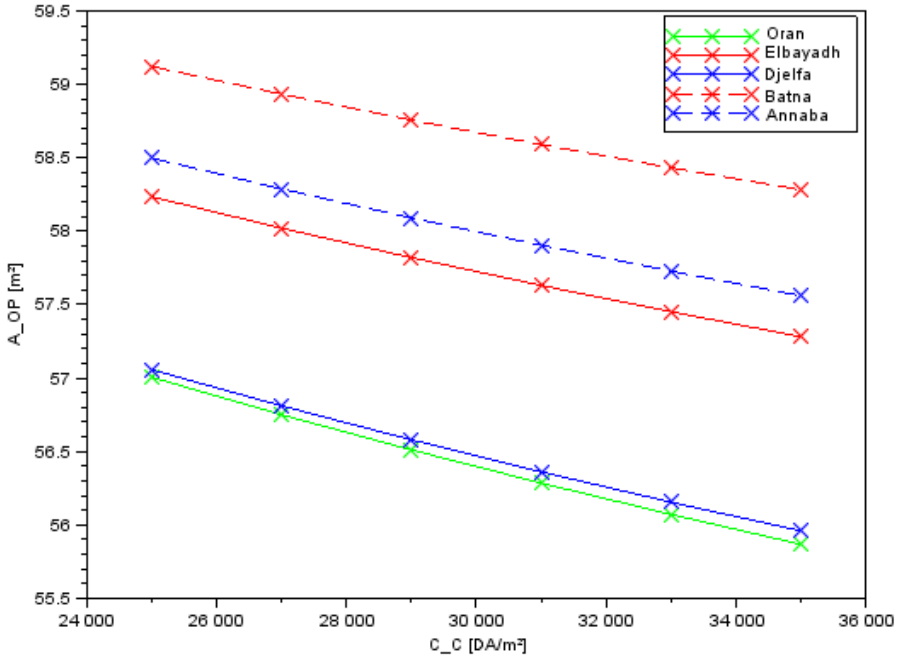

Figure II.15: optimal area variation vs the collector cost (1 m²) for different locations.

Figure II.16 represents the optimal surface variation according to the variation of unit electricity cost for five different locations: Elbayadh, Annaba, Oran, Djelfa and Batna. As much the auxiliary unit electricity cost, as much is better to replace it by solar energy, which mean increasing the collector surface by the same or even less cost estimated for auxiliary energy during the service.

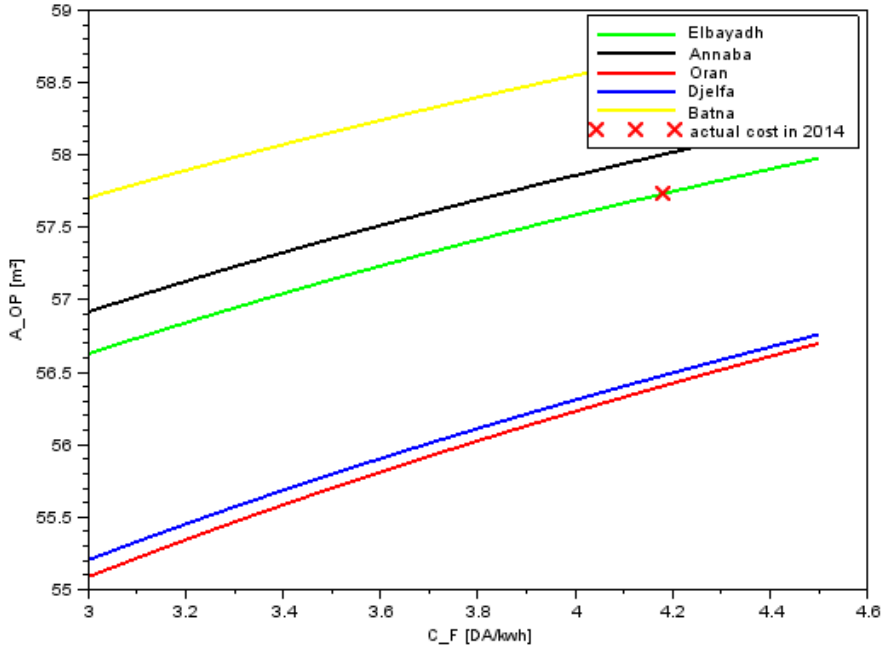

Figure II.16: optimal area variation vs C_F for different locations.

3.3 Application for the Industry case

An industrial process heat system has a 100 m² collector. The system is located in Ouargla (31° 57′ 47″ N latitude), and the collector characteristics are $F_R U_L = 4.5\ W/m^{2\circ}C$, $F_R\ (\tau\alpha\ )_n = 0.85, F'_R/F_R = 0.95$, tilted at 31° (south orientation). The process requires heat at a rate of 20 kW at a temperature of 70 °C for 8 h each day. The Specific storage is 120 $Kg\ m^{-2}$of water and the tank has an overall loss coefficient $(US)_S$=14 WK^{-1}. The heat exchanger has effectiveness $\varepsilon_L = 0.75$ and $C_{min} = 5000\ WK^{-1}$.

The heat required is given by

$$L=L_{req} \times \Delta t_h \qquad \text{(II.12)}$$

3.3.1 Conception results

Results are reported in the following figures:

Figure II.17 shows the industrial process heat demand during the 12 months of the year, it's clear that the variation is trivial, and that is because the way we define the heat demand, which is multiplying the capacity of the system by the duration of using which is stable every day, These variations are caused by the different number of days for each month.

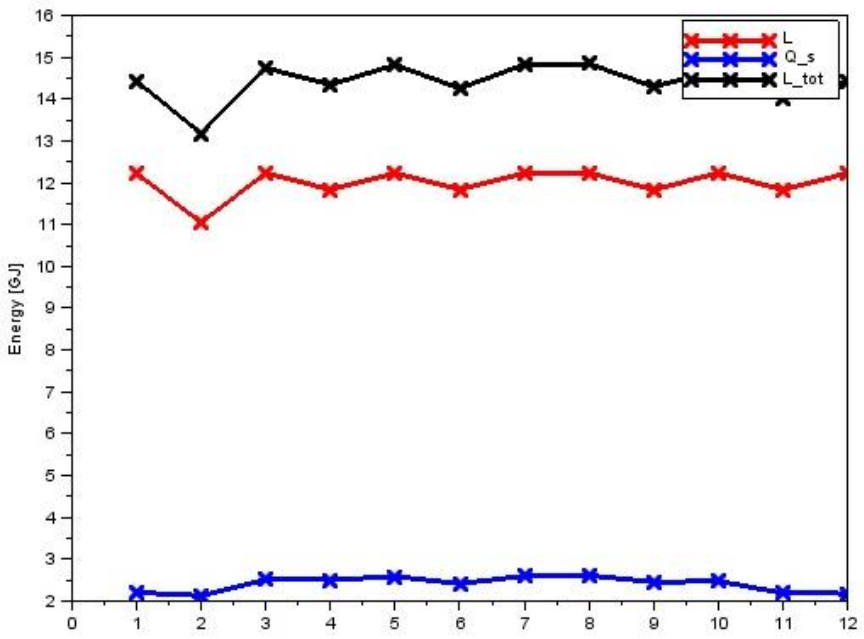

Figure II.17: Numerical results during the 12 months L,Q_S, L_{tot}.

The figure II.18 describe the monthly performances of the solar thermal system, we may notice that the highest fraction for the industrial process is reached in July. This is due to the maximum value of the incident solar radiation.

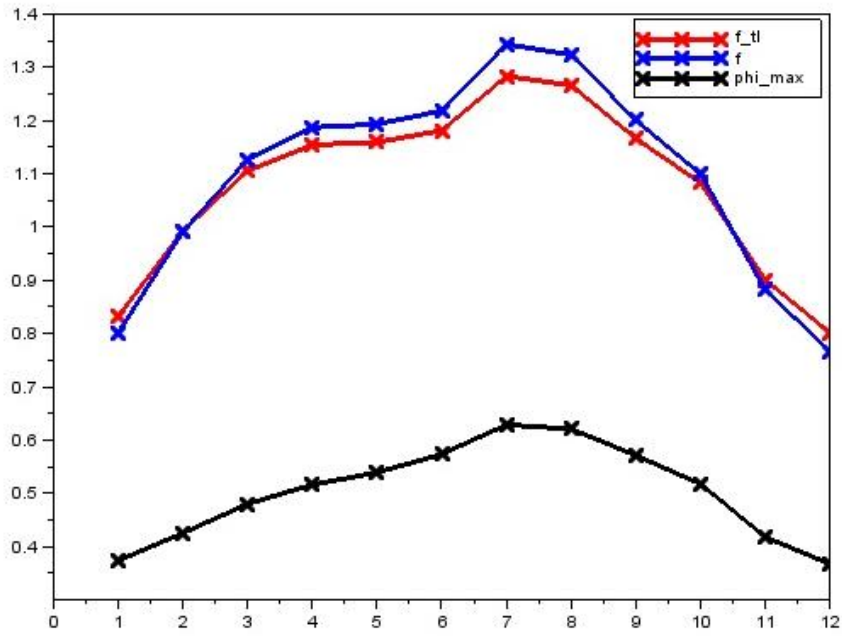

Figure II.18: Numerical results during the 12 months of for $f, f_{tl}, \bar{\Phi}_{max}$.

Figure II.19 shows the monthly variation of: the temperature of the inlet collector fluid, useful energy temperature, monthly average storage tank temperature, where the ambient temperature affects the rest of the temperatures mentioned.

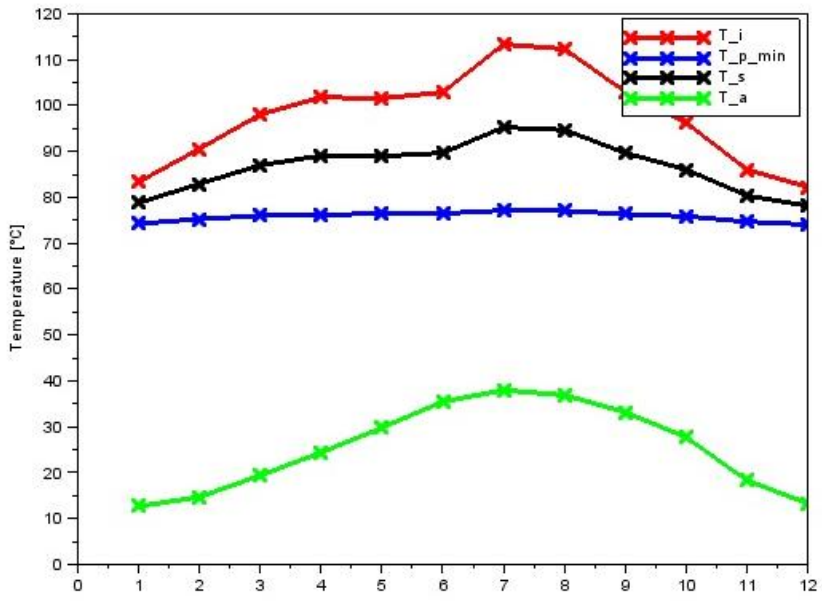

Figure II.19: Numerical results during the 12 months for $T_i, T_{p,min}, T_s, T_a$.

In figure II.20 we can see the variation of the two dimensionless parameters X which represents the energy losses, Y which represents the energy gain of the collector, $\bar{X}_c$ dimensionless average daily critical level of the solar collector, $\bar{X}_{c,min}$ minimum of the

dimensionless average daily critical level of the solar collector , all the variation are related to the incident solar radiation.

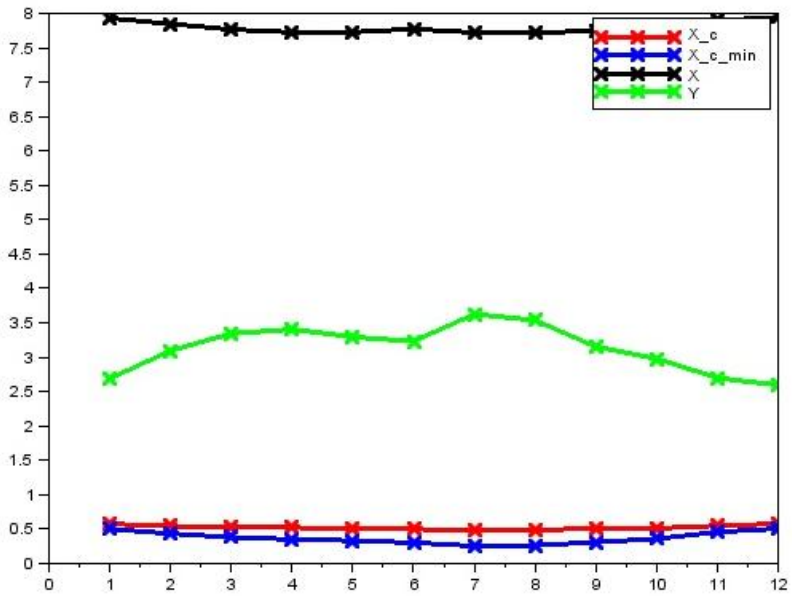

Figure II.20: Numerical results during the 12 months for X, Y, $\bar{X}_c, \bar{X}_{c,min}$.

Figure II.21 show the monthly average daily total solar radiation on a horizontal surface for Ouargla city, the measurement of monthly average daily extraterrestrial solar radiation and clearness index shows (see equation I-7) that the maximum monthly radiation in Ouargla is reached in July.

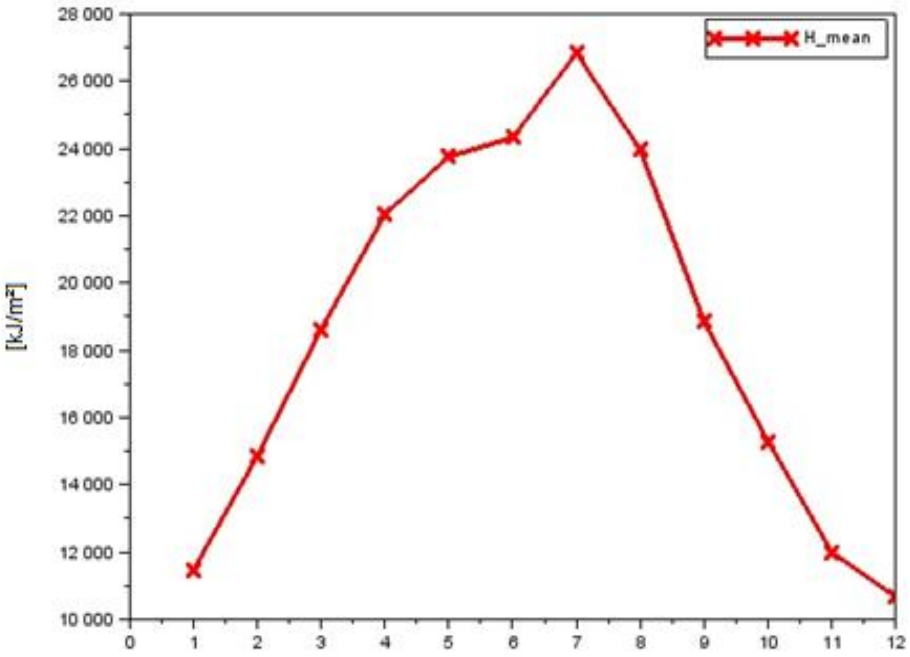

Figure II.21: Numerical results during the 12 months for $\bar{H}$.

3.3.2 Varying the parameters: (Industry case)

In this second section, we also provide some results about parameters variation. The previous example is simulated here by varying one parameter at once. The following figures report the solar fraction for hot water production during the year.

Figure II.22 shows the solar fraction during the year for three different collecting areas: 80 m², 90m² and 100m². It is evident that increasing the collecting area, the faction increases. Moreover we may notice that the highest fraction in Ouargla is reached in July. This is due to the maximum value of the incident solar radiation.

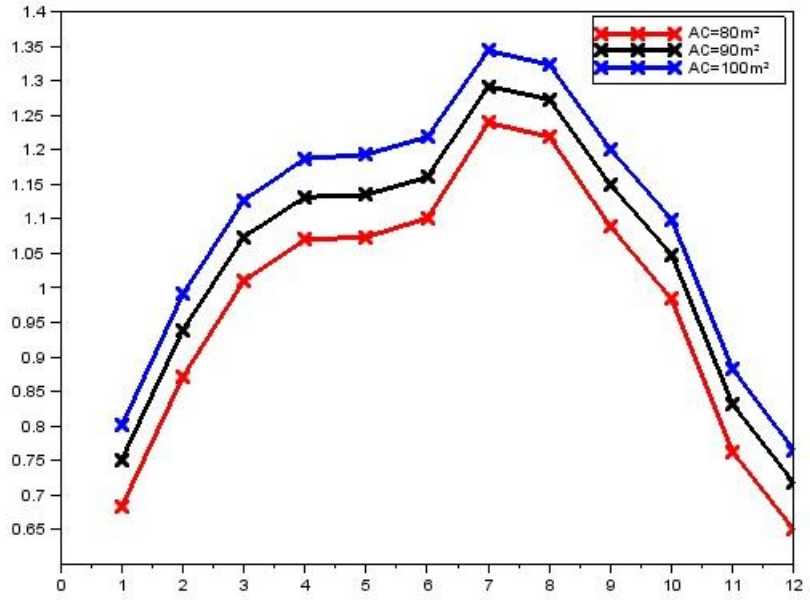

Figure II.22: Solar fraction with different collecting areas.

Figure II.23 describes the behavior of the solar fraction during the year for three different tilt angles of the solar collector: 20°, 31° and 40°. It is visible that configurations with lower angles are better during the summer and higher values of angles are better during the winter. This is due to the sun's apparent position during the year. In few words, this means that a fixed tilt angle cannot be optimal for all the months and that an automatic change in the inclination could be advisable.

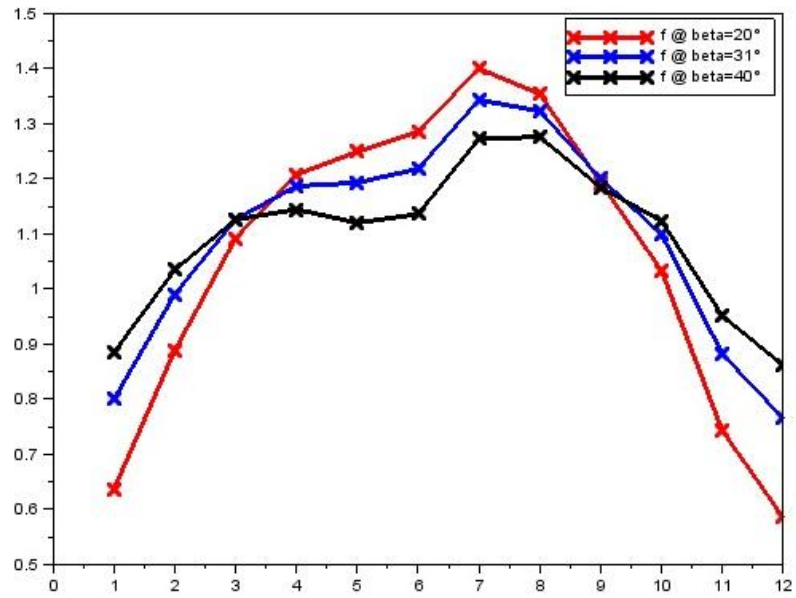

Figure II.23: Solar fraction with three different tilt angles of solar collector.

Figure II.24 contains the last set of experiments that have been carried out by changing the minimum required temperature. The experiments have been done for three different values: 65°C, 70°C and 75°C. The effect is simple all year round, the less the requirement, the higher the solar fraction.

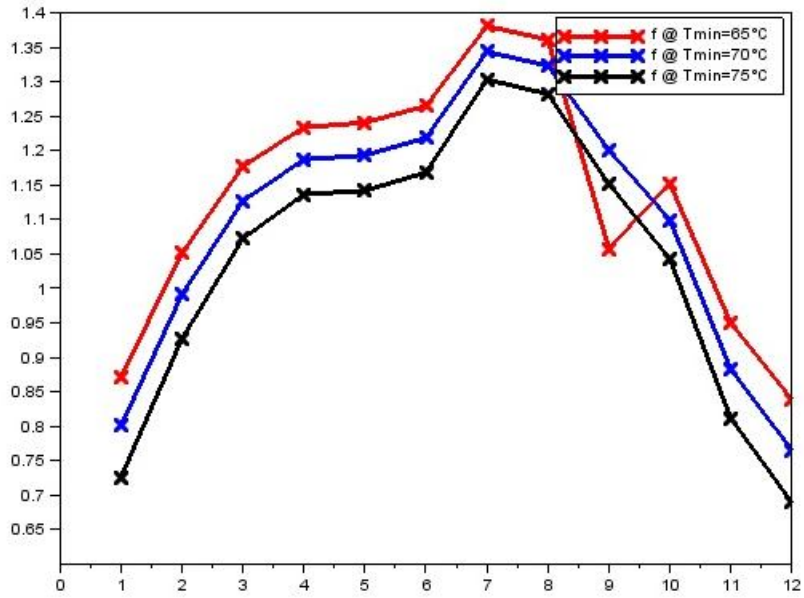

Figure II.24: Solar fraction with different minimum temperature requirements.

Figure II.25 shows the optimal area variation vs the collector cost (1m²), Where we used the formula (II.9) for the industrial process in Ouargla. We may notice the high cost of the collector effect on the optimal area. The results means that as much as the collector cost keep rising as much as it is advisable to compensate the energy obtained from the difference area between the optimal and the proposed one by the auxiliary energy to get the best economic benefit, (the economic parameters are already fixed as the same with the previous case).

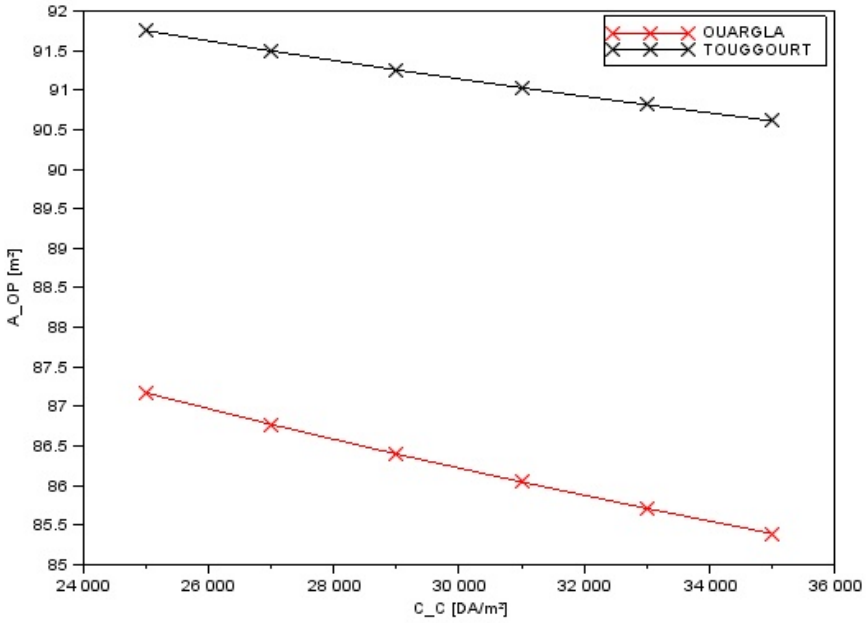

Figure II.25: Optimal area variation vs the collector cost for the two locations.

In the following two figures we plotted the annual auxiliary energy according the collecting area, for Ouargla and Touggourt application, with the same collector area and the same desired temperature, it's evident that a big collector area mean less auxiliary energy requirement.

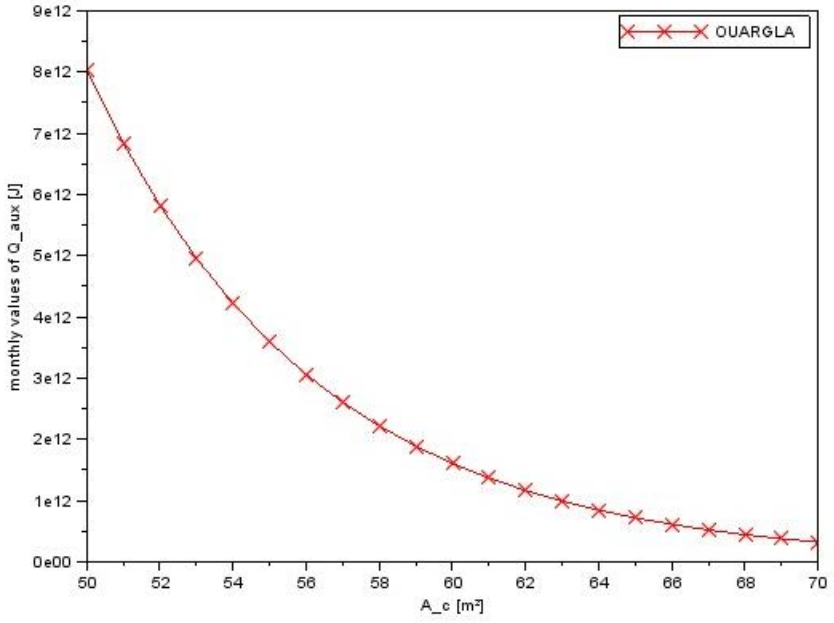

Figure II.26: Auxiliary energy required vs. collector area city of Ouargla.

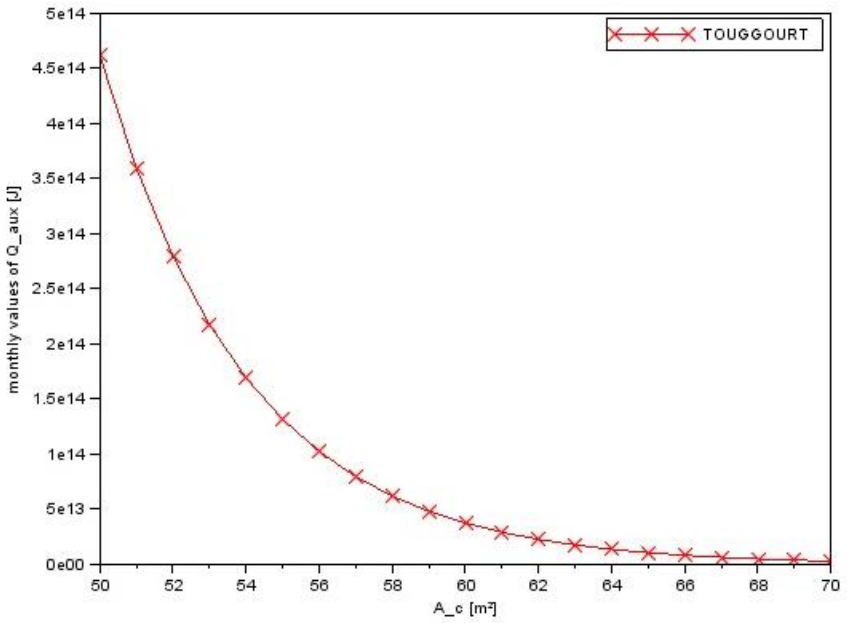

Figure II.27: Auxiliary energy required vs. collector area city of Touggourt.

We can see in figure II.28 that there is no requirement for auxiliary energy for the heat process from February to min-October.

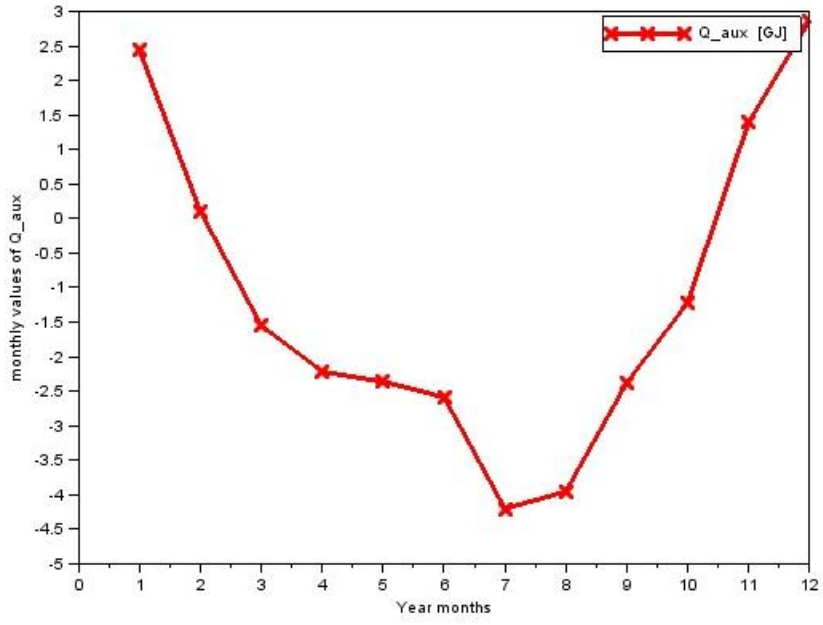

Figure II.28: Monthly variation of auxiliary energy required for city of Ouargla.

Figure II.29 represent the variation of the optimal area according to unit cost of electricity for the two locations Ouargla and Touggourt. The results means that, as much the auxiliary unit electricity cost, as much as it's better to replace it by the solar energy, which

means increasing the collector surface by the same or even less cost estimated for auxiliary energy during the service.

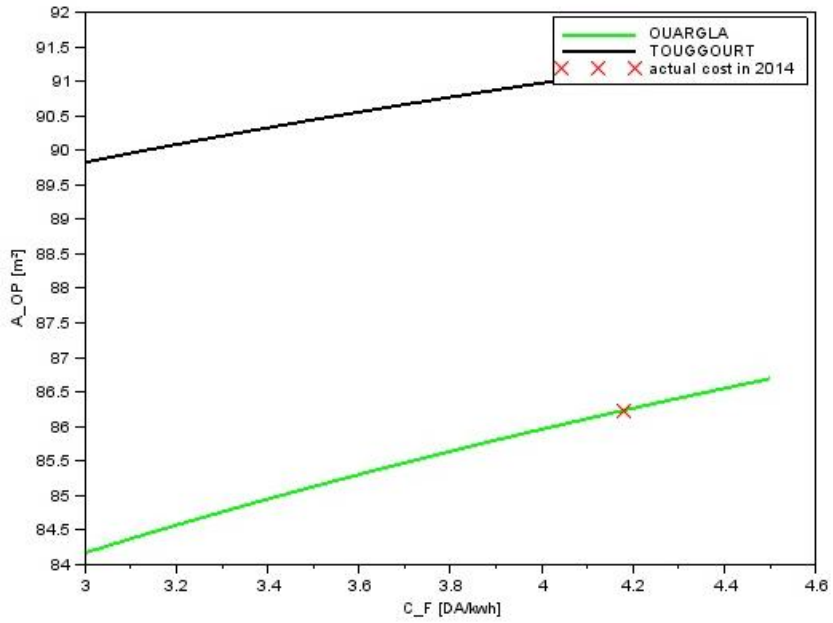

Figure II.29: Optimal area variation vs C_F for the two Wilaya.

The following two figures are combined by the results in figures II.25 and II.29.

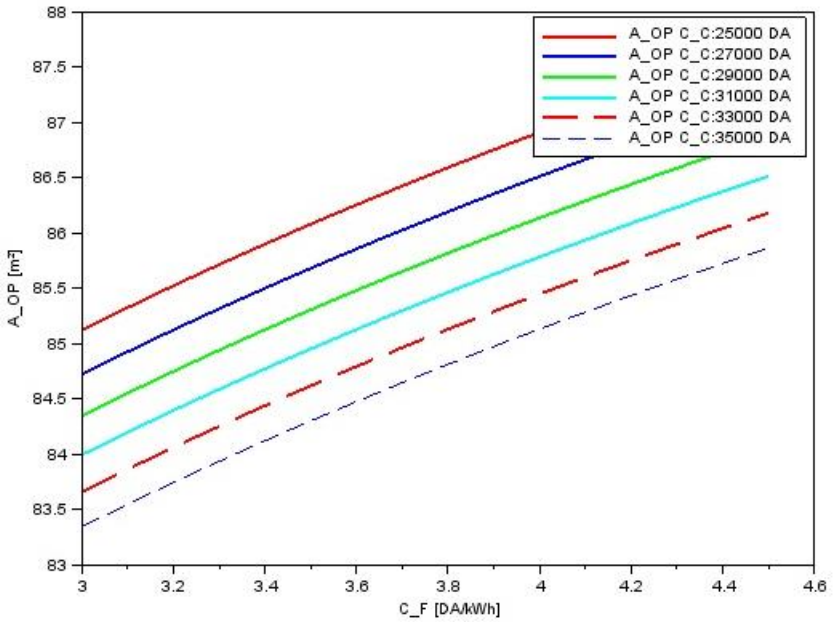

Figure II.30: Optimal area variation vs C_F with different collector prices for Ouargla.

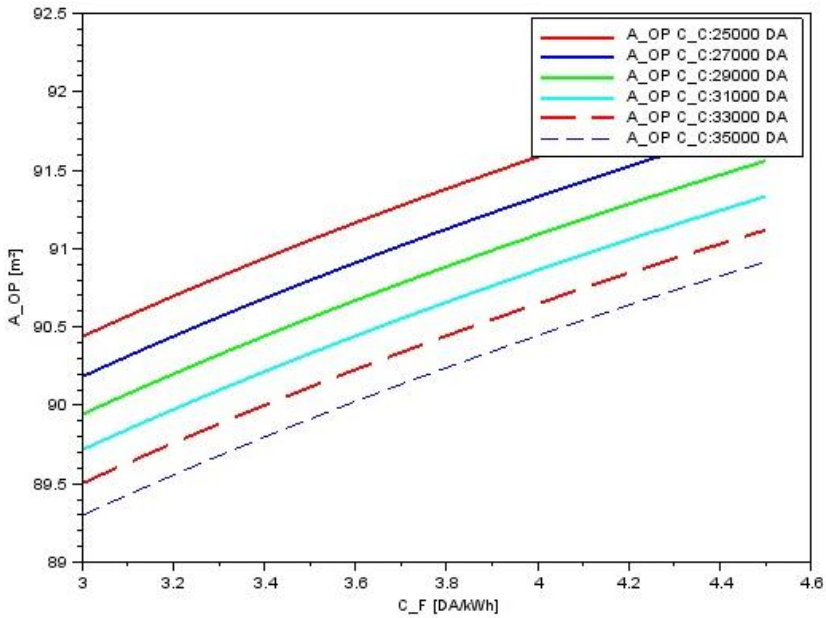

Figure II.31: Optimal area variation vs. C_F with different collector prices for Touggourt.

4. Conclusion

The results are completely parameterized and very fast. The advantage of having such a kind of model is that it may return within few seconds all relevant system quantities necessary to calibrate an optimal system. The results are about parameters variation and simulated by varying one parameter at once, which report the solar fraction for hot water production during the year.

General conclusion

In this master thesis, we describe and model the φ-f chart method with Scilab for optimize the design of active solar heating systems. The φ-f chart method is a simulation technique used in solar energy systems for heating and cooling. This method is particularly useful for sizing system components. The difficulty of sizing system's components lies in the fact that these systems are influenced by both predictable data (e.g. collectors, storage tanks …) and unpredictable data such as weather data.

This method is particularly useful in the simulation of absorption refrigerators, industrial process heating, and space heating systems where the thermodynamics cycle efficiency is independent of the heat supply temperature.

This system is composed by a solar collector array designed to collect heat by absorbing sunlight. After, the heat is transferred to the storage tank through a heat exchanger which separates the fluid used in the solar collector from water contained in the storage tank. Then the heat is transferred to the load through a circuit with an auxiliary heater that possibly compensates to reach the minimum required temperature.

The design of the solar heating systems use optimal solar collector area, which is defined as the area that optimizes the system from both economic and thermal performance aspects. This area is the result of a cost-benefit approach. In this work, we introduced a mathematical model for the determination of optimal collector area of the solar installations of collective water heating. This method is based on a minimization of the total cost of the installation. This by holding account, not only costs of the various components and price of the conventional energy consumed by the auxiliary system, but also of the thermal performances of the installation starting.

The results are completely parameterized and very fast. The advantage of having such a kind of model is that it may return within few seconds all relevant system quantities necessary to calibrate an optimal system. The results are about parameters variation and simulated by varying one parameter at once, which report the solar fraction for hot water production during the year.

The presented study can intended to be integrated with optimization algorithms to design the most appropriate solar energy systems at the minimum cost.

Bibliography

[1] A. Duffie, W. A. Beckman, “Solar Engineering of Thermal Processes”, John Wiley & Sons, 1991.

[2] S. Kalogirou, Solar energy engineering, processes and systems, Academic Press 2009.

[3] Soteris A. Kalogirou, “Solar thermal collectors and applications, Progress in Energy and Combustion Science 30 (2004) 231–295.

[4] SOLAR PHYSICS AND TERRESTRIAL EFFECTS, Space Environment Center.

[5] Outils Solaires (Energie solaire thermique) [online], (2014) Available on: http://outilssolaires.com/developpement-durable/energie-solaire/ (Consulted 08/04/2014).

[6] F. Bagui et H. Chafouk, Etude transitoire du système solaire thermique, Revue des Energies Renouvelables CER’07 Oujda (2007), p.99 – 102.

[7] Hauguel Energy, [online], (2014) Available on: http://www.hauguelenergy.com/ifr2c52-fonctionnement-du-panneau-solaire-tubulaire.htm (Consulted 24/04/2014).

[8] M. Capderou. Atlas solaire de l’Algérie. Tome 1 et 2. Alger : Office des publications universitaires, 1986, 399p.

[9] M. Koussa, M. Haddadi et A. Malek, “Effet à long terme de la poursuite sur les performances d’un système de chauffe-eau solaire “ Revue des Energies Renouvelables Vol. 15 N°2 (2012) 249 – 264.

[10] Minister of Natural Resources, Clean Energy Project Analysis: RETSCREEN Engineering & Cases Textbook, Canada 2001 – 2004.

[11] I. F. Okafor and G. Akubue , F-Chart Method for Designing Solar Thermal Water Heating Systems, International Journal of Scientific & Engineering Research Volume 3, Issue 9, September-2012.

[12] Electropaedia [online], (2014) Available on: http://www.mpoweruk.com/solar_power.htm, (Consulted 27/05/2014).

[13] WELEM - L’entreprise (solaire thermique) [online], (2014) Available on : http ://www.welem.com/wre/solaire/solaireThermiqueSoluce.shtml, (Consulted 24/04/2014).

[14] Girando Industries , [online], (2014) Available on : http://www.giordano.fr/chauffage-solaire-giordano-pour-piscine-individuelle (Consulted 24/04/2014).

[15] Saunier Duval Algerie, [online], (2014) Available on: http://duval.algerie.prix-construction.info/construction_neuve/ (Consulted 04/06/2014).

[16] S.Sami-Mecheri, A.Hamid, N. Ait Messaoudenne and M. Belhamel, Etude de la Rentabilité d'une Installation Solaire de Chauffage d'Eau Collective Application à Différents Sites Algériens, 11èmes Journées Internationales de Thermique (2003)53-57.

[17] KWEI-KWANG CHANG and ANTONIO MINARDI, AN OPTIMIZATION FORMULATION FOR SOLAR HEATING SYSTEMS, Pergamon Press Ltd., 1980. Printed in Great Britain, Solar Energy Vol. 24, P. 99 to 103.

[18] Scilab enterprises, [online], (2014) available on: http://www.scilab.org/en, (Consulted 04/06/2014).

Appendix

Numerical data:

Results are reported in the following tables:

Wilaya	DATA	Jan	Feb	Mars	April	Mai	Juin	July	Aug	Sept	Oct	Nov	Dec
Ouargla (31.57°)	T_{min}	4	7	9	14	18	23	26	25	22	16	10	6
	T_{max}	17	20	23	29	33	39	43	42	37	31	23	18
	T_a	12.7	14.7	19.4	24.4	29.8	35.5	38	36.9	33.2	27.7	18.3	13.3
	$\bar{H}_0$	19430.37	24350.836	30529.537	36741.733	40965.412	42671.66	41933.88	38643.268	33068.502	26369.827	20681.492	18095.231
	K_T	0.59	0.61	0.61	0.60	0.58	0.57	0.64	0.62	0.57	0.58	0.58	0.59
Elbayadh (33.41°)	T_{min}	0	1	4	7	12	17	21	20	16	11	5	2
	T_{max}	10	12	16	19	24	31	35	34	28	22	15	10
	T_a	5	6.5	10	13	18	24	28	27	22	16.5	10	6
	$\bar{H}_0$	17695	21089	26650	33383	38393	41084	41376	39422	35082	29023	22549	18333
	K_T	0.5597	0.6031	[0.6050	0.6207	0.6190	0.6245	0.6247	0.5992	0.6142	0.5991	0.5469	0.5574
Oran (35.63°)	T_{min}	5	7	9	10	14	17	20	21	18	14	10	7
	T_{max}	17	18	20	22	25	28	31	31	29	26	21	18
	T_a	11.5	12.5	14.5	16	19.5	22.5	25.5	26.5	23.5	20	14.5	12.5
	$\bar{H}_0$	16485	19941	25679	32761	38167	41161	41509	39341	34619	28188	21458	17138
	K_T	0.5778	0.6136	0.6081	0.6274	0.5465	0.6224	0.6247	0.6131	0.5984	0.5728	0.5645	0.5591
Batna (35.75°)	T_{min}	0	1	3	6	10	15	18	18	14	10	5	1
	T_{max}	12	14	17	20	26	32	35	35	29	24	17	13
	T_a	6	7.5	10	13	18	23.5	26.5	26.5	21.5	17	11	7
	$\bar{H}_0$	16410	19870	25619	32722	38152	41164	41516	39335	34590	28136	21390	17065
	K_T	0.5481	[0.5970	0.5998	0.6040	0.6049	0.6140	0.6397	0.6176	0.5926	0.5909	0.5569	0.5496
Djelfa (34.33°)	T_{min}	0	1	4	6	11	16	19	19	15	10	5	2
	T_{max}	10	12	16	18	24	30	34	33	27	22	15	11
	T_a	5	6.5	10	12	17.5	23	26.5	26	21	16	10	6.5
	$\bar{H}_0$	17288	20704	26326	33178	38321	41114	41425	39399	34930	28746	22183	17931
	K_T	0.5586	0.6160	0.6105	0.6188	0.6179	0.6227	0.6306	0.6032	0.5989	0.5993	0.5664	0.5706
Annaba (36.83°)	T_{min}	2	2	5	7	12	16	18	19	16	12	6	3
	T_{max}	12	14	17	20	26	31	35	34	29	24	17	13
	T_a	7	8	11	13.5	19	23.5	26.5	26.5	22.5	18	11.5	8
	$\bar{H}_0$	15742	19231	25071	32361	38009	41190	41573	39273	34317	27661	20780	16404
	K_T	0.5471	0.5640	0.5810	0.5838	0.5988	0.6113	0.6412	0.6255	0.5744	0.5632	0.5243	0.5151
Touggourt (33.07°)	T_{min}	5	6	10	14	19	24	26	26	23	17	10	6
	T_{max}	17	20	24	28	33	38	41	41	36	30	23	18
	T_a	11	13	17	21	26	31	33.5	33.5	29.5	23.5	16.5	12
	$\bar{H}_0$	18064	21437	26941	33566	38454	41053	41329	39439	35216	29272	22879	18696
	K_T	0.6413	0.6724	0.6443	0.6457	0.6317	0.6486	0.6486	0.6375	0.6042	0.6188	0.6172	0.6369

Table 1: cities data.

Month	$\bar{H}$	$\bar{K}_T$	$\bar{R}$	R_n	$(\tau\alpha)_n$	Ta	L
1	9,90E+03	0,56	1,47	1,36	0,91	5	1,50E+10
2	1,27E+04	0,60	1,33	1,27	0,91	7	1,35E+10
3	1,61E+04	0,61	1,15	1,15	0,91	10	1,36E+10
4	2,07E+04	0,62	1,01	1,05	0,90	13	1,13E+10
5	2,38E+04	0,62	0,91	0,98	0,89	18	8,85E+09
6	2,57E+04	0,62	0,87	0,96	0,89	24	5,17E+09
7	2,58E+04	0,62	0,89	0,97	0,89	28	2,77E+09
8	2,36E+04	0,60	0,96	1,02	0,90	27	2,79E+09
9	2,15E+04	0,61	1,09	1,11	0,91	22	5,28E+09
10	1,74E+04	0,60	1,26	1,22	0,91	17	8,39E+09
11	1,23E+04	0,55	1,41	1,32	0,91	10	1,13E+10
12	1,02E+04	0,56	1,53	1,40	0,90	6	1,39E+10

Table 2: Elbayadh numerical data

month	X_c	$X_{c,min}$	X	Y	$\bar{\Phi}_{max}$	T_i	$T_{p,min}$	T_s	L_{tot}	Q_s	f	f_{tl}
1	0,52	0,50	4,51	1,30	0,39	60,39	57,83	59,11	1,65E+10	1,47E+09	0,43	0,48
2	0,47	0,44	4,53	1,52	0,43	62,39	58,67	60,53	1,49E+10	1,37E+09	0,56	0,60
3	0,44	0,39	4,90	1,82	0,48	65,87	59,38	62,62	1,52E+10	1,60E+09	0,74	0,77
4	0,43	0,34	5,53	2,29	0,53	72,54	59,91	66,22	1,30E+10	1,68E+09	0,96	0,96
5	0,46	0,30	6,92	2,94	0,57	82,01	59,52	70,77	1,08E+10	1,90E+09	1,17	1,14
6	0,54	0,24	9,99	4,35	0,64	100,3	58,46	79,43	7,21E+09	2,05E+09	1,49	1,35
7	0,64	0,20	14,46	6,49	0,70	121,6	57,35	89,48	5,15E+09	2,38E+09	1,94	1,51
8	0,65	0,20	14,17	6,34	0,70	123,7	57,36	90,56	5,25E+09	2,46E+09	1,94	1,50
9	0,55	0,23	9,55	4,47	0,67	110,3	58,67	84,50	7,54E+09	2,27E+09	1,54	1,38
10	0,48	0,28	7,12	3,12	0,61	90,36	59,58	74,97	1,05E+10	2,06E+09	1,25	1,20
11	0,46	0,39	5,57	1,92	0,50	68,13	59,10	63,62	1,29E+10	1,58E+09	0,80	0,83
12	0,49	0,46	4,84	1,49	0,43	62,33	58,35	60,34	1,54E+10	1,51E+09	0,55	0,60

Table3: Elbayadh numerical results

Month	$\bar{H}$	$\bar{K}_T$	$\bar{R}$	R_n	$(\tau\alpha)_n$	Ta	L
1	1,16E+04	0,64	1,58	1,44	0,92	11	1,22E+10
2	1,44E+04	0,67	1,40	1,32	0,92	13	1,10E+10
3	1,74E+04	0,64	1,18	1,18	0,92	17	1,22E+10
4	2,17E+04	0,65	1,02	1,07	0,91	21	1,18E+10
5	2,43E+04	0,63	0,91	0,99	0,90	26	1,22E+10
6	2,66E+04	0,65	0,87	0,96	0,89	31	1,18E+10
7	2,68E+04	0,65	0,89	0,97	0,90	34	1,22E+10
8	2,51E+04	0,64	0,97	1,03	0,91	34	1,22E+10
9	2,13E+04	0,60	1,10	1,12	0,91	30	1,18E+10
10	1,81E+04	0,62	1,30	1,25	0,92	24	1,22E+10
11	1,41E+04	0,62	1,51	1,39	0,92	17	1,18E+10
12	1,19E+04	0,64	1,65	1,48	0,91	12	1,22E+10

Table 4: Touggourt data

month	X_c	$X_{c,min}$	X	Y	$\bar{\Phi}_{max}$	T_i	$T_{p,min}$	T_s	L_{tot}	Q_s	f	f_{tl}
1	0,55	0,48	7,92	2,91	0,37	84,55	74,54	79,54	1,45E+10	2,23E+09	0,85	0,87
2	0,53	0,44	7,87	3,20	0,40	88,60	75,17	81,89	1,31E+10	2,10E+09	0,97	0,97
3	0,53	0,41	7,83	3,23	0,43	91,88	75,53	83,70	1,46E+10	2,39E+09	1,04	1,03
4	0,52	0,37	7,77	3,42	0,48	97,47	76,07	86,77	1,43E+10	2,42E+09	1,14	1,12
5	0,51	0,35	7,75	3,38	0,51	99,13	76,24	87,69	1,48E+10	2,54E+09	1,17	1,14
6	0,50	0,31	7,76	3,51	0,55	104,34	76,66	90,50	1,43E+10	2,45E+09	1,25	1,21
7	0,49	0,28	7,76	3,62	0,59	109,38	76,95	93,16	1,47E+10	2,52E+09	1,30	1,25
8	0,50	0,27	7,69	3,72	0,61	114,27	77,15	95,71	1,49E+10	2,65E+09	1,34	1,28
9	0,52	0,30	7,66	3,59	0,58	111,77	76,91	94,34	1,45E+10	2,63E+09	1,30	1,24
10	0,52	0,32	7,65	3,61	0,55	109,61	76,75	93,18	1,50E+10	2,74E+09	1,27	1,22
11	0,53	0,39	7,77	3,31	0,48	98,08	75,94	87,01	1,43E+10	2,43E+09	1,11	1,09
12	0,54	0,44	7,86	3,08	0,41	89,34	75,14	82,24	1,46E+10	2,33E+09	0,96	0,97

Table 5: Touggourt numerical results

Month	$\bar{H}$	$\bar{K}_T$	$\bar{R}$	R_n	$(\tau\alpha)_n$	Ta	L
1	9,66E+03	0,56	1,51	1,39	0,91	5,00	3,01E+09
2	1,28E+04	0,62	1,36	1,29	0,92	6,50	2,70E+09
3	1,61E+04	0,61	1,16	1,16	0,91	10,00	2,72E+09
4	2,05E+04	0,62	1,00	1,05	0,90	12,00	2,34E+09
5	2,37E+04	0,62	0,90	0,98	0,89	17,50	1,81E+09
6	2,56E+04	0,62	0,86	0,95	0,89	23,00	1,11E+09
7	2,61E+04	0,63	0,88	0,96	0,89	26,50	6,40E+08
8	2,38E+04	0,60	0,96	1,02	0,90	26,00	6,40E+08
9	2,09E+04	0,60	1,09	1,11	0,91	21,00	1,13E+09
10	1,72E+04	0,60	1,28	1,24	0,91	16,00	1,70E+09
11	1,26E+04	0,57	1,46	1,36	0,91	10,00	2,27E+09
12	1,02E+04	0,57	1,58	1,44	0,91	6,50	2,75E+09

Table 6: Djelfa data (5 m² collector area, 7 persons,"Orraset mark")

month	X_c	$X_{c,min}$	X	Y	$\bar{\Phi}_{max}$	T_i	$T_{p,min}$	T_s	L_{tot}	Q_s	f	f_{tl}
1	0,11	0,11	0,25	0,31	0,84	55,72	55,03	55,37	3,96E+09	9,47E+08	0,02	0,26
2	0,10	0,09	0,25	0,37	0,86	56,01	55,13	55,57	3,56E+09	8,61E+08	0,10	0,32
3	0,09	0,08	0,27	0,42	0,88	56,31	55,18	55,74	3,67E+09	9,57E+08	0,15	0,37
4	0,08	0,08	0,29	0,50	0,89	56,81	55,24	56,02	3,27E+09	9,34E+08	0,22	0,45
5	0,07	0,07	0,36	0,63	0,90	57,81	55,25	56,53	2,78E+09	9,79E+08	0,32	0,56
6	0,07	0,06	0,48	0,86	0,92	61,32	55,29	58,30	2,02E+09	9,15E+08	0,58	0,77
7	0,07	0,05	0,61	1,14	0,93	71,23	55,29	63,26	1,64E+09	9,98E+08	1,04	1,02
8	0,07	0,05	0,60	1,13	0,93	70,86	55,28	63,07	1,66E+09	1,02E+09	1,01	1,01
9	0,06	0,05	0,46	0,88	0,92	62,43	55,32	58,87	2,08E+09	9,56E+08	0,62	0,80
10	0,07	0,06	0,37	0,68	0,91	58,86	55,29	57,08	2,69E+09	9,93E+08	0,39	0,62
11	0,08	0,08	0,30	0,46	0,88	56,65	55,17	55,91	3,20E+09	9,31E+08	0,16	0,41
12	0,10	0,10	0,27	0,36	0,86	56,03	55,09	55,56	3,71E+09	9,52E+08	0,07	0,31

Table 7: Djelfa numerical results (5 m² collector area, 7 persons, "Orraset mark")

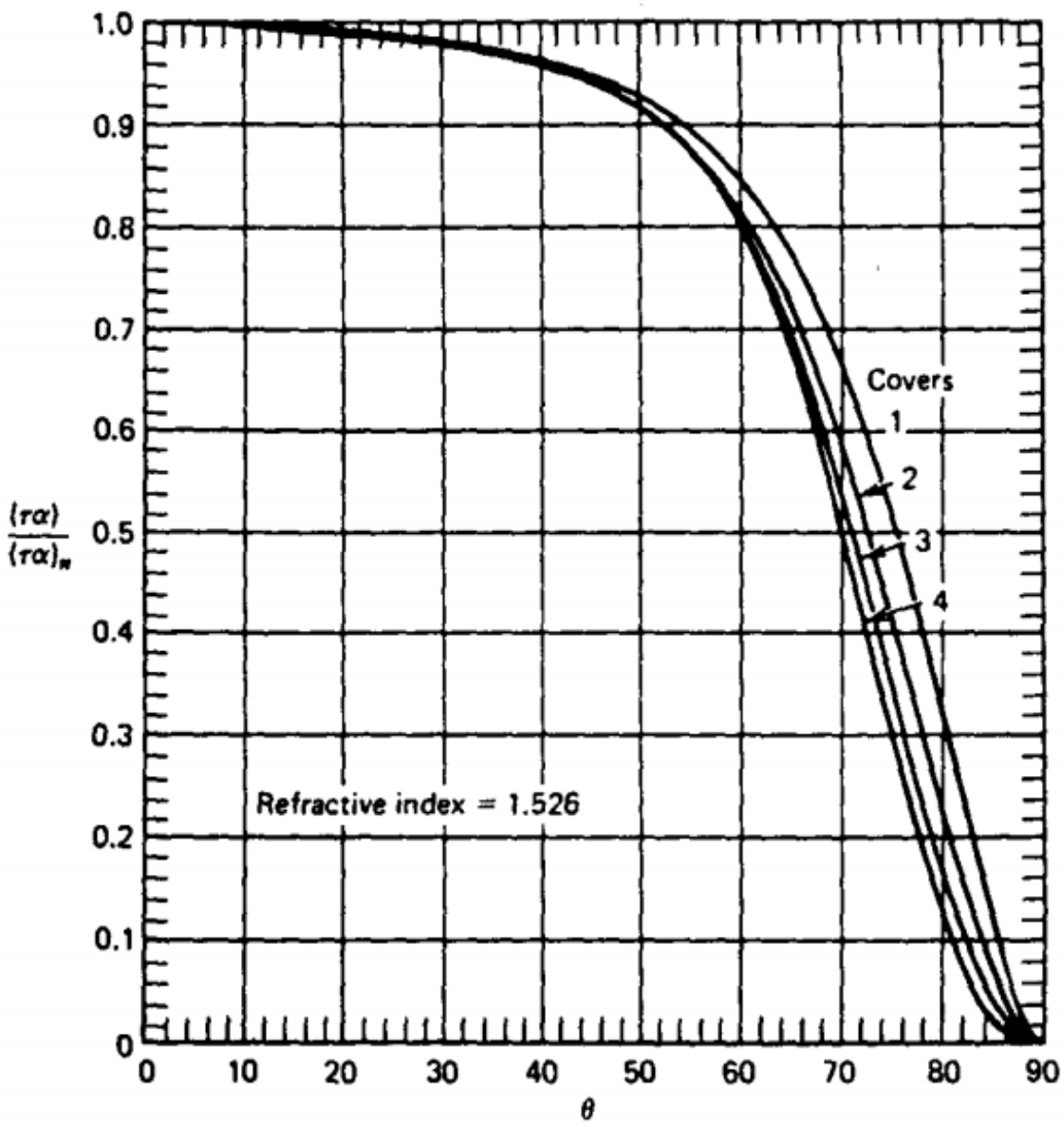

Figure 1: Typical $(\overline{\tau\alpha}\,)/\,(\tau\alpha\,)_n$ curves for I to 4 covers. Adapted from Klein (1979) [1].

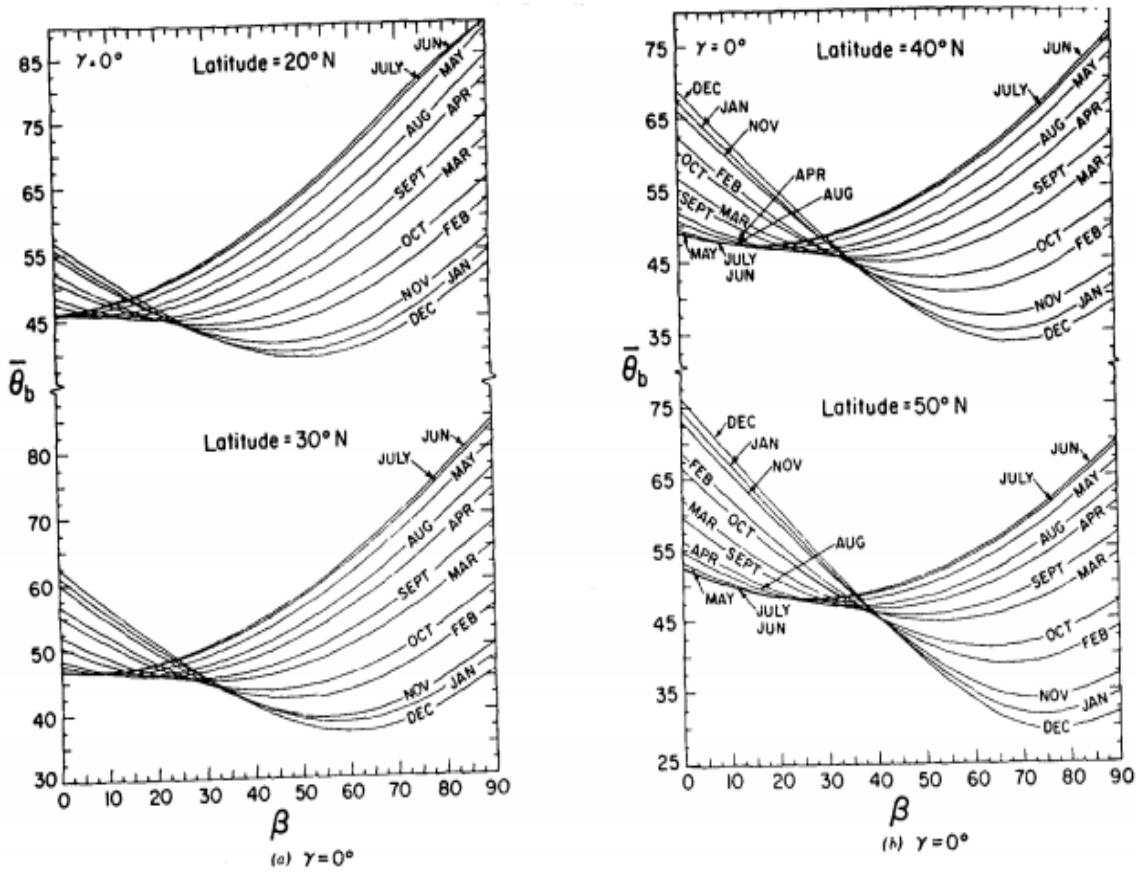

Figure 2: Monthly average beam incidence angle for various surface locations and orientations. For southern hemisphere interchange months [1].

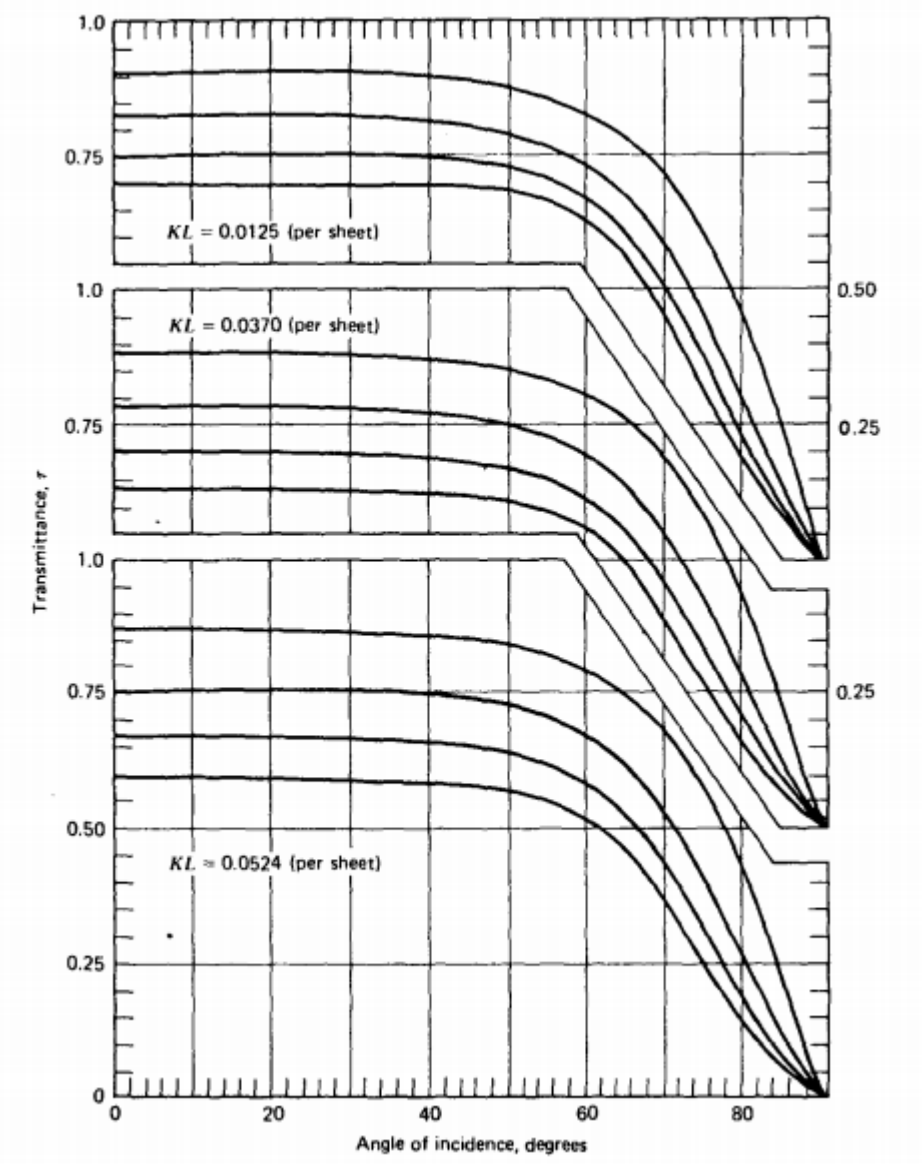

Figure 3: Transmittance (considering absorption and reflection) of 1. 2. 3 and 4 covers for three types of glass [1].

ملخص:

تؤثر احتياجات الطاقة في المباني على تصميم أنظمة الطاقة المتجددة، لذلك فمن المهم جدا تحسين أداء طاقة في المباني أولاً، ثم تحليل مختلف مصادر الطاقة المتجددة التي يمكن إستخدامها.

قمنا في هذه الدراسة بتحسين أداء كود حساب لتقدير إحتياجات الطاقة في المباني القائمة على نظم الطاقة الشمسية الحرارية. وذلك بإستخدام طريقة الكسور الشمسية لنمذجة المعطيات المختلفة. تم دمج أمثلية متعددة الأهداف في تصميم النظام، والتي تمكن من تصميم أنظمة طاقة شمسية مناسبة بأقل تكلفة.

الكلمات المفتاحية: نظام طاقة شمسية، بنايات ذات إحتياجات منخفضة للطاقة، كود تصميم, أمثلية متعددة الأهداف.

Résumé :

Les besoins d'énergie des bâtiments ont une influence sur la conception des systèmes d'énergie renouvelable, il est donc très important d'abord d'optimiser la performance énergétique des bâtiments et après d'analyser les différentes sources d'énergie renouvelable qui pourraient être ajoutées.
Nous aurons développé un outil de calcul pour estimer les besoins énergétiques des bâtiments basé sur les systèmes d'énergie solaire thermique. Le code utilise la méthode des fractions solaire pour la modélisation des différents paramètres. Une optimisation multicritère est intégrée dans la conception du système, ce qui permet de concevoir des systèmes d'énergie solaire appropriées au moindre coût.

Mot Clés :

Système d'énergie solaire, Bâtiments à basse consommation, outil de conception, optimisation multicritère.

Abstract:

The energy requirements for buildings have an influence on the design of renewable energy systems, it is very important to optimize the energy performance of buildings first, then after analyzing the various renewable energy sources that could be added.

We have developed a calculation tool for estimating the energy requirements of buildings based on solar thermal energy systems. The code uses the solar fractions method for modeling different parameters. Multicriteria optimization is integrated into the system design, which enables to appropriate least-cost solar energy systems.

Key word:

Solar power system, low energy buildings, tool design, multicriteria optimization.